Improved anti-melanoma and anti-melanogenic effects of birch bark triterpenes delivered in ethosomes

A thesis presented to

The Faculty of Graduate Studies

of

Lakehead University

by

STATTON EADE

In partial fulfillment of requirements
for the degree of
Master of Science in Biology

March 26th, 2018

Abstract

North American birch species of the boreal forest contain significant amounts of pentacyclic triterpenes in their outer bark. Betulin (BE) and betulinic acid (BA), pentacyclic triterpenes readily extracted from outer birch bark, have been reported to exhibit a wide array of therapeutic effects, including selective inhibition against melanoma, and the inhibition of key enzymes involved in skin aging and melanogenesis. Despite their promising therapeutic effects and lack of toxicity towards healthy cells, their use in pharmaceuticals and cosmetics has been limited by their poor hydrosolubility. Ethosomes are lipid vesicles that have been successfully employed to encapsulate hydrophobic compounds and enhance their drug delivery and bioavailability. The aim of this study was to investigate the use of ethosomes as a delivery system for triterpenes and evaluate their anti-melanoma and anti-melanogenic effects. BE, BA, and a triterpene extract from *Betula papyrifera* (TE) were successfully incorporated into an ethosome for the first time and assessed for their anti-melanoma and anti-melanogenic effects in B16-F10 melanoma cells. Firstly, ethosomes containing BE, BA, or TE were prepared and characterized by their vesicle size, entrapment efficiency, and morphology. The cytotoxicity on B16-F10 melanoma cells was then explored. Lastly, the effect on cellular tyrosinase activity in B16-F10 cells was evaluated as a measure of anti-melanogenic effect. The ethosomal triterpenes had mean vesicle sizes ranging from 3.67 – 5.11 μm and high entrapment efficiencies ranging from 93.25 – 95.76%. The ethosomal triterpenes showed significant cytotoxicity and higher *in vitro* anti-melanoma effects than triterpene solutions of equivalent concentration. BE-ethosomes showed an IC_{50} of 2.43 μM compared to 14.38 μM in BE solutions. BA-ethosomes showed an IC_{50} value of 3.07 μM compared to 16.41 μM in BA solutions. TE (IC_{50} = 36.00 μg/mL) showed cytotoxicity comparable to both BE and BA, but its effect was not improved by the ethosomal solution (IC_{50} = 43.51 μg/mL). BE, BA, and TE showed significant anti-melanogenic effect, inhibiting tyrosinase more effectively than the standard inhibitor kojic acid. These findings support the use of BE, BA, and TE as therapeutic agents and outlines their potential for topical and transdermal applications for the treatment of melanomas and skin aging.

Lay Summary

Faculty and students in the Department of Biology are bound together by a common interest in explaining the diversity of life, the fit between form and function, and the distribution and abundance of organisms. This research was undertaken to better understand the functions and therapeutic potential of naturally occurring secondary metabolites produced by *Betula papyrifera.* Compounds such as betulin and betulinic acid have promising therapeutic potential and are readily extracted from low-value tree bark residues from the forestry industry, though are often over-looked on account of their poor hydrosolubility. By studying their *in vitro* biological effects on cancer cell populations, and attempting to enhance their delivery and bioavailability through novel drug delivery systems, these compounds may prove useful in the development of naturally sourced therapies to treat a range of human diseases. This work represents the first investigation of ethosomal nanocarriers as a delivery system for the triterpenes betulin and betulinic acid. Ethosomes were shown to incorporate these triterpene compounds with high efficiency, and enhance their anti-melanoma effect as demonstrated on B16-F10 melanoma cells. Further, the ethosomal triterpenes showed higher anti-melanogenic effect than the positive control kojic acid.

Acknowledgements

I would first and foremost like to thank my supervisor Dr. Sudip Rakshit who has been an exceptional mentor to me throughout my studies. His wisdom, kindness, and support have been invaluable to me during my research. I would like to thank my co-supervisor, Dr. Zacharias Suntres, for his valuable input in the development of my research, and providing me direction and guidance in regards to drug delivery systems. I thank Brian Garhofer of The Actives Factory for his generous donation of materials, without which my research would not have been possible, and for his valuable input to the direction of my work. I thank all of my fellow lab members of the Biorefining Research Institute, who made my long days enjoyable and fostered a sense of community and camaraderie within our lab: Sai Swaroop Dalli, Bijaya Kumar Upretty, Amit Nair, Benazeer Ali, Mahdieh Samavi, Ibtisam Sharif, Hanin Alhazimi, and Peter Adewale. My thanks to Christina Richard, who has been a mentor and a friend throughout my studies, and has always allowed me to voice my opinions. I thank Jaclyn Brown for her unwavering love and support, and for always keeping me grounded. I thank Bruce and Lucille Brown for being a second family to me. Above all I would like to thank my parents Lindsay and Joanne Eade, who have given me their love and supported me unconditionally through the most difficult of times. From childhood to this day, they have forged my character, my compassion, and my values. They have consistently put themselves second to allow me the best chance of achieving a better station in life. I will never be able to repay them for everything they have done and continue to do for me. I dedicate this study to them.

Abbreviations

BA - Betulinic acid

BE - Betulin

DMEM - Dulbecco's modified Eagle's medium

DMSO – Dimethyl sulfoxide

DNA – Deoxyribonucleic acid

DPPC – Dipalmitoylphosphatidylcholine

E-BE – Ethosomal betulin

E-BA – Ethosomal betulinic acid

E-TE – Ethosomal triterpene extract

EE - Entrapment efficiency

EtOH - Ethanol

FBS – Fetal bovine serum

HIV – Human immunodeficiency virus

HPLC – High pressure liquid chromatography

KA – Kojic acid

L-DOPA – L-3,4-dihydroxyphenylalanine

MTO – Mitoxantrone

MTT - 3-(4,5-dimethylthiazol-2-yl)-2,5-diphenyltetrazolium bromide

PBS – Phosphate buffered saline

PFTE - Polytetrafluoroethylene

PPE – Porcine pancreatic elastase

PR – Phenylethyl resorcinol

RCF – Relative centrifugal force

ROS – Reactive oxygen species

SD – Standard deviation

SEM – Scanning electron microscopy

TE – The Actives Factory Triterpene Extract

UV – Ultraviolet

Table of Contents

List of Tables

List of Figures

1 - Introduction

Melanomas are a form of skin cancer characterized by early metastasis, rapid development, poor prognosis, and high mortality [1]. Despite early detection, surgical resection, and adjuvant therapies, the number of new cases and melanoma-related deaths continues to rise. Melanomas are one of the most therapy-resistant malignancies, and the few drugs that are approved for treatment of melanoma are often attributed with adverse side effects [2]. Betulin and betulinic acid are pentacyclic triterpenes found in significant quantities in the outer bark of *Betula papyrifera* and other species of North American birch. These compounds have been shown to exhibit selective cytotoxicity towards melanoma cells through the induction of apoptosis [3]–[5]. Accompanied by their lack in toxicity towards normal cells, these compounds represent promising anti-tumour agents. Despite their distinct bioactive properties, their use towards the development of pharmaceutical therapies and cosmetics has been limited by their poor aqueous solubility. A drug delivery system which has been employed to enhance delivery and uptake of hydrophobic compounds is the ethosome. Ethosomes are a type of multilayer lipid vesicle characterized by their high ethanol content (20-45%), with high potential for the development of topical applications for skin disease therapies. Ethosomes are capable of encapsulating both hydrophilic and hydrophobic compounds, like triterpenes, and delivering them into the deep layers of the skin more efficiently than traditional liposomes [6], [7]. Furthermore, ethosomes have recently been shown to enhance the anti-melanoma and anti-melanogenic effect of certain compounds [1], [8]. In this study, ethosomes containing betulin, betulinic acid, and a standardized triterpene extract from outer bark of *Betula papyrifera* developed by The Actives Factory were prepared and evaluated for their cytotoxicity towards melanoma cells and their anti-melanogenic effects. This work aims to add to the research being conducted on the development of safer, non-invasive, and naturally sourced melanoma therapies free from adverse side effects.

1.1 – Skin Cancer and Melanoma

Skin cancer is the most common form of cancer in Canada. The combined number of new melanoma and non-melanoma skin cancer cases in 2018 will nearly match that of the four major cancers combined (lung, breast, colorectal, prostate) [9] . The three main types of skin cancer, named according to the cell type from which they arise, are basal cell carcinoma, squamous cell carcinoma, and melanoma of the skin. The more common but less deadly skin cancers are known as non-melanoma skin cancers: squamous cell carcinoma and basal cell carcinoma. The third type, melanoma, is the deadliest form of skin cancer, and although it represents only 4% of all skin cancer diagnoses, it is responsible for 75% of all skin cancer-related deaths. Melanoma on its own accounts for about 3% of all new cancer cases, placing it in the top 10 cancers diagnosed in Canada [10]. Because most cases are identified early, it represents only 1.4% of all cancer deaths. Despite increased public awareness, the incidence rates of melanoma have increased for both males and females over the past decades, rising by 2.1% per year in males and 2.0% per year in females between 1992 and 2013 [10]. The slow-rising rates of melanoma mean greater efforts are required to encourage sun protection and restrict use of artificial tanning sources.

Melanomas are malignant tumours that arise from neural crest-derived melanocytes which are pigmented cells found in the epidermis and sometimes the dermis [11]. The process in which melanocytes progress to malignant melanomas involves a series of steps, beginning with the development of benign naevocellular naevus, preneoplastic dysplastic naevus, primary melanoma, and finally metastatic melanoma [12]. The four types of melanoma are superficial spreading melanoma, nodular melanoma, lentigo maligna melanoma, and acral lentiginous melanoma [13]. The most common type is superficial spreading melanoma, which accounts for approximately 70% of reported melanoma cases, while nodular melanoma accounts for 15-30%, lentigo melanoma 4-10%, and acral lentiginous melanoma 2-8% of melanoma cases [14].

1.1.1 - Risk Factors

The risk factors for development of cutaneous melanoma are both environmental and genetic. The predominant environmental factor leading to melanoma, as well as non-melanoma skin cancers, is exposure to UV radiation, which accounts for 90% of melanoma cases in North America [15]. The most at risk individuals are those who experience intermittent sun exposure, such as individuals who work indoors but spend free time outdoors and whose skin is not well-adapted to the sun, as well as those with a history of severe sun burns, as the risk of developing melanoma is increased two-fold in those who have had ten or more severe sun burns [16], [17]. Exposure to artificial UV radiation from tanning beds and sun lamps also increases the risk of developing melanoma, as UV light emitted from tanning beds was classified as a human carcinogen in 2009 by the World Health Organization International Agency for Research on Cancer [18]. Contrary to claims from the indoor tanning industry, artificial tanning is neither a safe or useful way to increase systemic vitamin D levels [19]. The use of indoor tanning beds can increase an individual's risk of developing squamous cell carcinoma by 67%, basal cell carcinoma by 29%, and melanoma by 20% [20], [21]. Skin pigment also plays an important role in melanoma susceptibility, as there is an inverse correlation between melanoma risk and the degree of skin colour from light to dark, which arises from the protective role that melanin plays against UV damage to human skin [22]. Features such as fair skin, freckling, blue or green eyes, blonde or red hair, are all risk factors for the development of melanoma [17], [23].

1.1.2 - Treatment and Prevention

The key to skin cancer prevention is through minimizing exposure to harmful levels of UV radiation, which includes avoiding artificial sources of UV radiation such as tanning beds and using proper sun protection when exposed to sunlight. Current methods for the treatment of metastatic melanoma include surgery [24], isolated limb perfusion [25], cryotherapy [26], radiation therapy [27], BRAF inhibition [28], as well as several immunotherapies in various stages of drug development [29]–

[32]. Although patients diagnosed with malignant melanoma have excellent prognosis when treated at early stages, current treatments such as chemotherapy and immunotherapy are unsatisfactory in managing advanced melanoma cases, and thus improved and/or combined treatments are required.

1.2 - Skin Aging

Aging is a complex phenomenon that has been defined by biologists as the sum of all changes that occur in a living organism throughout its life that contribute to the decreased ability to survive stress, functional impairment, and ultimately death [33]. Skin aging is determined by both intrinsic (genetic) and extrinsic (environmental) factors and is therefore defined by two types: chronological aging, and photo-aging. Chronological aging is determined primarily by intrinsic factors and hormonal status, while photo-aging is the result of exposure to environmental aggressors such as UV radiation, chemical agents, and stress [34], [35]. Both types of aging leads to dry and thin skin, wrinkles, age spots, and degradation of the collagen and elastin fibers in the skin. Wrinkle and age spot formation are believed to be primarily induced by UV radiation, and therefore long-term skin care solutions for topical application are of great interest for physicians and patients alike.

1.2.1 - Wrinkles

The process of skin aging involves the deterioration of skin tissue and structural changes to the macromolecules of the extracellular matrix of the dermis [36]. Elastin is a major component the elastic fibers that form a candelabra type network in the papillary dermis, which give the skin its elastic properties but progressively degrade over time as a result of decreased synthesis and increased degradation of elastin fibers due to exposure to UV radiation [37]. Thus, over time, the skin loses its elasticity and wrinkles become more prevalent. The only enzyme that is capable of degrading elastin is elastase, and therefore inhibition of this enzyme can be considered a useful strategy for protecting against skin aging resulting from UV radiation [38].

1.2.2 - Hyperpigmentation

Another common condition observed in photo-aged skin are localized hyperpigmented regions known as age spots. Age spots are clinically diagnosed as solar lentigines, and represent a localized increase in pigmentation, which may be a result of increased number of melanocytes or an increase in melanin pigment [39]. Melanin is the pigment responsible for the colour of skin, hair, and eyes. It is produced in cells called melanocytes which are located in the bottom layer of the epidermis and middle layer of the eye through a process called melanogenesis. Tyrosinase, a multifunctional copper-containing enzyme, regulates melanogenesis within melanocytes. It catalyzes the hydroxylation of tyrosine to L-3,4-dihydroxyphenylalanine (L-DOPA) and the oxidation of L-DOPA to dopaquinone, which is converted to melanin after a series of reactions involving cyclization and oxidative polymerizations [40]. Thus, tyrosinase is responsible for the pigmentation of skin, hair, and eyes in mammals. The over-activity of tyrosinase induced by UV radiation can lead to the development of both melanoma and age spots, and therefore one mechanism which has been employed to decrease pigmentation is inhibition of the enzyme tyrosinase by compounds such as hydroquinone, arbutin, and kojic acid [41]–[43]. Although these anti-melanogenic agents and others like retinol (vitamin A) are currently used as topical agents to treat hyperpigmentation, they can often lead to adverse effects in the form of skin irritation, and raise concerns for safety regarding long-term exposure [44]. As a result, patients and consumers alike are increasingly shifting their interest towards the use of natural depigmenting agents for their high tolerability, efficacy, and easily accessible formulations.

1.3 – North American White Birch (*Betula papyrifera*)

The utilization of bioactive compounds from natural sources has long been an area of focus in research, but there has been little attention given to trees of the northern boreal forests. One tree which has garnered attention in the past few decades is white birch. *Betula papyrifera*, commonly known as white birch or paper birch, is a medium sized deciduous tree native to northern North America. It is

distributed throughout all provinces and territories in Canada, with the exception of Nunavut, as well as northern regions of the United States of America including Alaska. The *Betula* species exhibit various therapeutic properties and have been used in traditional medicines in many parts of the world throughout history. One of the more common uses was in the treatment of ailments relating to the bones such as arthritis, rheumatism, and gout, while the sap has been used to treat rashes, hepatitis, and scurvy [45]. The outer bark has also long been the subject of folk remedies. Birch bark oil has been used in folk medicine for the treatment of skin diseases such as eczema and psoriasis [46], while Native Americans prepared teas from the bark for the treatment of digestive tract infections [47]. The outer bark of boreal birch species has now been shown to contain considerable amounts pentacyclic triterpenes, a class of plant secondary metabolite with proven therapeutic properties. These compounds can account for upwards of 35% of the dry weight of the outer bark, which is the highest quantity found in any known plant [48].

The Canadian and American forestry industries produce massive amounts of residues annually in the form of stems, sawdust, leaves and bark from commercially managed species such as birch. Though rich in bioactive compounds such as triterpenes, these residues are typically burned as fuel to reduce energy costs. The current demand for these compounds is still growing, but in future years these compounds could very well satisfy requirements for pharmaceuticals, cosmetics, fungicides, biocides, as well as yet to be developed markets, since the supply of natural bark sources is virtually unlimited. Finding economical, naturally sourced products from abundant low-value raw materials such as forestry residues can bring added value to the forestry industry and the bioeconomy, while providing safe, effective, and natural alternatives for pharmaceutical and cosmetic development.

1.4 - Birch Bark Triterpenes:

Terpenes are a group of plant secondary metabolites that have been extensively researched due to their wide range of bioactive properties. Triterpenes, a class of terpene, consist of six isoprene units and arranged in complex cyclic structures [49]. Pentacyclic triterpenes consist of a 30-carbon skeleton

composed of 5 six-membered rings (ursanes and lanostanes) or 4 six-membered rings and 1 five-membered ring (lupanes and hopanes) (Figure 1). Triterpenes are ubiquitously distributed throughout the Plant Kingdom with high potential as bioactives. Their physiological function in plants is believed to be as a defence against plant pathogens [48], which makes them an interesting candidate for potential defence against human and animal disease. Although factors such as their low aqueous solubility and relatively high molecular weight have traditionally limited their attractiveness for use in the drug industry, their established low toxicity and high efficacy supports their use in drugs, cosmetics, dietary supplements, biocides, and more [50].

The outer bark of boreal birch contains an extremely high content of pentacyclic triterpenes including betulin (BE), betulinic acid (BA), lupeol, betulinic caffeates, and betulinic aldehyde. Among triterpenes, BE is one of the most abundant in nature, and is responsible for the characteristic white colour of birch bark, where it is found in crystalline deposits in the outermost layers and nearly fills the interior of the peridermal cells. [51]. Betulin and betulinic acid have been shown to exhibit anti-inflammatory, anti-cancer, and anti-viral properties and have great potential for pharmaceutical and cosmetic development.

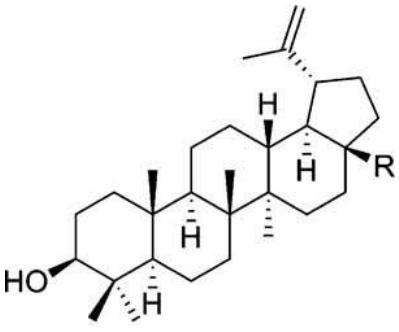

R = CH_2OH betulin
R = COOH betulinic acid

Figure 1: Chemical structure of the lupane-type triterpenes betulin and betulinic acid.

1.5 - Betulin

Betulin (3*β*-28-dihydroxylup-20(29)-ene), a pentacyclic lupane-type triterpene, was first isolated from the bark of white birch in 1788, making it one of the first natural products to be isolated and scientifically described (Figure 1) [48]. It occurs in a variety of plant species and in particularly high concentrations in the outer bark of many birch species including *Betula papyrifera* (white birch)*, Betula pendula* (silver birch)*, Betula alba* (downy birch)*,* and *Betula alleghaniensis* (yellow birch). In these species, BE can account for 20-30% of the dry weight of the outer bark, with the levels influenced by a variety of factors including the species of birch, its regional location, and the overall health and age of the tree [52]. Though in lesser quantities, BE can also be found in the roots and leaves of birch species [53]. Like other members of the triterpene family, BE exhibits antifungal and antimicrobial effects, and likely serves as a defence to fungal and bacterial attack through the bark. Along with these properties, BE also exhibits a wide range of other properties important to human health including anti-inflammatory [54], anti-viral and anti-HIV[47], hepatoprotective [55], and anti-cancer activity [56], [57]. Despite its wide range of bioactivities, the anti-cancer and chemopreventive potential of BE has garnered the most attention. The cytotoxic and anti-proliferative effects of BE have been described for a variety of cell lines of human cancers (Table 1), with the degree of effect depending on the cancer cell type, ranging from strong inhibition of cell proliferation in human neuroblastoma cells (SK-N-AS) with an IC_{50} (concentration of drug which results in 50% reduction in cell growth) value of 2.5 μM, to a far less pronounced effect against human myelogenous leukemia cells (K562) with an IC_{50} value of >250 μM. Furthermore, there is often a great deal of variation in the degree of inhibition of cell proliferation between studies on the same cell lines. For example, BE has been studied extensively on the A549 human lung cancer cell line, with IC_{50} values ranging from 3.8 μM [58], 7.4 μM [59], 20 μM [60], to 33.4 μM [61].

Table 1: Cytotoxic effects of BE and BA on human and animal cancer cell lines.

Compound	Cancer Type	Cell Line	IC_{50} (μM)	Reference
Betulin	Human lung carcinoma	A549	33.4	[61]
			20.0	[60]
			7.4	[59]
			3.8	[58]
	Human melanoma	G631	12.4	[62]
		SK-MEL-28	16.2	[62]
		MEL-2	>45.2	[5]
		SK-MEL-2	>250.0	[66]
	Mouse melanoma	B16-F10	13.8	[63]
		B16-2F2	27.4	[64]
	Human neuroblastoma	GOTO	17.1	[62]
		NB-1	16.5	[62]
		SK-N-AS	2.5	[59]
	Human leukemia	U937	14.4	[62]
		HL60	14.7	[62]
		K562	>250	[66]
	Human breast adenocarcinoma	MCF-7	8.32	[67]
	Human colorectal adenocarcinoma	DLD-1	6.6	[63]
Betulinic Acid	Human lung carcinoma	A549	10.3	[63]
	Human melanoma	G361	5.2	[62]
		SK-MEL-28	6.5	[62]
	Mouse melanoma	B16-F10	16.1	[63]
		B16-2F2	7.9	[64]
	Human neuroblastoma	GOTO	7.9	[62]
		NB-1	9.5	[62]
	Human leukemia	HL60	6.6	[62]
		U937	10.0	[62]
		K562	9.8	[62]
	Human breast adenocarcinoma	MCF-7	>50	[68]
	Human colorectal adenocarcinoma	DLD-1	15	[63]

IC_{50} = concentration of drug at which cell growth was inhibited by 50%

1.5.1 - Anti-Melanoma Activity

The cytotoxic activities of BE against several melanoma cell lines have been tested with promising results. The IC_{50} values of BE in human melanoma cells SK-MEL-28 (16.2 μM) and G631 (12.4 μM) [62], were similar to that of murine melanoma cells B16-F10 (13.8 μM) [63], but much lower than that of murine melanoma cells B16 2F2 (27.4 μM) [64] and human melanoma cells MEL-2 (45.2

μM) [5]. This would suggest that the anti-proliferative potential of BE is independent of whether the cell is of human or non-human origin. In another murine melanoma cell line, B16-4A5, BE showed a 52% reduction in viable cells compared to the control at a concentration of 10 μM [65], compared to moderate activity in epidermoid mouth carcinoma KB cells with an IC_{50} value >45 μM [5], and inactivity towards SK-MEL2 cells with an IC_{50} value >250 μM [66].

1.5.2 - Mechanisms of Action

The induction of apoptosis, a type of programmed cell death characterized by a series of complex biochemical events, is an essential mechanism for anti-cancer agents, and has been shown to be one of the mechanisms leading to the cytotoxic and anti-proliferative effects of BE [69]. Cytomorphological alterations such as cell rounding, chromatin condensation, membrane blebbing, nuclear condensation/fragmentation, and apoptotic body formation are indicative of cells undergoing apoptosis, and have been observed in cells treated with BE [61]. The treatment of murine melanoma B164A5 cells with BE resulted in nearly equivalent proportions of apoptotic and dead cells among affected cells [65]. In addition, a study by Mullauer et al. (2009) investigating the effect of BE on Jurkat cells revealed BE induces mitochondrial damage that leads to cytochrome C release and apoptosis [70].

1.5.3 - Toxicity

BE, like many other pentacyclic triterpenes, has shown no toxicity. The minimal lethal dose and median lethal dose (LD50) in mice were reported as 6500 mg/kg and 9000 mg/kg, respectively [71]. Although there have been no published clinical trials using BE to treat cancer thus far, there have been studies using birch bark extract to treat actinic keratoses which have shown promising results [72], [73]. Actinic keratoses represent early and non-invasive squamous cell carcinoma induced by exposure to UV radiation in sunlight, and should be treated in order to prevent the development of non-melanoma skin cancers [74]. Huyke et al. (2009) incorporated a birch bark extract composed of 87% triterpenes (80%

BE) into an oleogel, which following a three-month treatment period resulted in >75% clearing of lesions in 86% of the patients, and 100% clearing of lesions in 64% of the patients [73].

1.6 - Betulinic Acid

Betulinic acid (3*β*-hydroxylup-20(29)-ene-28-oic acid), a C-28 carboxylic acid derivative of betulin, is potentially the most-studied of all pentacyclic triterpenes and has garnered significant attention in recent years due to its wide array of biological effects including anti-inflammatory, anti-HIV, and anti-cancer activities. It was first described by Retzlaff in 1902 as an unknown compound extracted from *Gratiola officinalis* [75], and later identified and named in 1939 by Robertson et. al [76]. It is found in a variety of plants, but much like BE, it occurs in particularly high quantities in the outer bark of white birch and other members of the Betulaceae family. Other reported sources of betulinic acid include *Ziziphus* spp. (Rhamnaceae) [3], *Diospyros* spp. (Ebenaceae) [77], *Syzygium* spp. (Myrtaceae) [78], *Uapaca* spp. (Euphoribiaceae) [79], and *Paeonia* spp. (Paeoniaceae) [80]. Unlike BE, the quantities of naturally occurring BA in plants have proven to be quite low. The synthesis of BA from BE, which is available in sufficient quantities from botanical sources, has been employed to meet the demands of BA for biological and clinical testing. Though earlier methods of synthesis gave low yields and small-scale preparations, improved methods developed in the past decade have led to simpler, more cost-effective routes of synthesis that can be achieved at an industrial scale [81], [82]. BA was initially discovered as a highly selective inhibitor of human melanoma growth through the induction of apoptosis, however subsequent studies reported anti-cancer activity against several other types of cancer including neuroectodermal tumors such as neuroblastoma, medulloblastoma, and glioblastoma, as well as carcinomas of the head, neck, colon, breast, lung, prostate, ovaries, and cervix [83]–[87].

1.6.1 - Anti-melanoma Activity

BA has been shown to have strongly selective anti-tumor activity against human and animal melanoma cells [88]. In a study of lupane-type triterpenes against murine melanoma (B16-F10), BA

showed similar anti-proliferative activity to BE, with IC_{50} value of 16.1 μM (compared to 13.8 μM for betulin) [63]. BA exhibited higher anti-proliferative activity when tested against human melanoma cell lines G361 and SK-MEL-28, with IC_{50} values of 5.2 μM and 6.5 μM, respectively [62]. In the same study, it was reported that the carbonyl group at C-17, and not the carboxylic acid group as previously suggested, plays an essential role in these inhibitory activities through the inhibition of topoisomerase I, an enzyme essential in the replication of DNA.

1.6.2 - Mechanisms of Action

BA's biological activity stems from several mechanisms, including the induction of apoptosis, antiangiogenesis, cell cycle arrest, immunoregulation, as well as autophagy induction [89]–[92]. There have been many studies demonstrating BA's ability to trigger apoptosis in cancer cells through disruption of mitochondrial membrane potential, the production of reactive oxygen species (ROS), as well as permeability transition pore openings which results in the release of mitochondrial apogenic factors, caspase activation, and DNA fragmentation [93]. The *in vitro* incubation of BA with melanoma cells led to the appearance of surface blebbing and cytoplasmic shrinking, both of which are characteristic of cells undergoing apoptosis [3].

1.6.3 – Toxicity

BA has been reported to show remarkably low toxicity, with no toxic effect in mice at concentrations as high as 500 mg/kg, in which doses were given intraperitoneally every fourth day for a total of six treatments [3]. Similarly, doses of 200 and 400 mg/kg of BA administered to rats showed no evidence of toxicity [94]. Several studies have also demonstrated that normal cells including human skin fibroblasts, peripheral blood lymphocytes, and melanocytes are much more resistant to BA than cancer cells[95], [96]. These findings suggest BA possesses minimal broad toxicity, if any, at therapeutic doses.

1.7 - The Actives Factory Triterpene Extract

The Actives Factory Triterpene Extract (TE) is a natural extract product manufactured by The Actives Factory, an active-ingredient manufacturer with a production facility located in Two Harbors, Minnesota, USA. They specialize in the extraction, isolation, purification, and synthesis of compounds such as betulin, betulinic acid, lupeol, and betulin caffeates from the outer bark of North American birch bark (*Betula papyrifera)* using unique extraction and processing technologies initially developed at University of Minnesota's Natural Resources Research Institute. Their triterpene extract is produced from the outer bark of *Betula papyrifera* and is especially suited for cosmetic and nutraceutical development, and contains a mixture of triterpenes including BE, BA, lupeol, betulinic aldehyde, and betulinic caffeates (Table 1.2). All birch bark used by The Actives Factory is paper milling waste product sourced from sustainably managed and harvested trees.

Table 2: Composition of The Actives Factory Triterpene Extract.

Compound	Content
Betulin	65%
Betulinic Acid	7%
Lupeol	7%
Betulinic Caffeates	19%
Betulinic Aldehyde	2%
Other	<0.5%

1.8 – Anti-aging and Anti-melanogenic Effects of Birch Bark Triterpenes

Birch bark triterpenes have also been shown to exhibit significant inhibitory activity against key enzymes involved in skin aging such as elastase, responsible for development of wrinkles, and tyrosinase, the key enzyme involved in melanogenesis and the development of hyperpigmentation/age spots. Compounds capable of counteracting these enzymes can be considered useful in skin-care and anti-aging formulations. In a study of elastase inhibitory properties of triterpenes extracted from *Meliosma oldhamii,* a deciduous tree native to China, Japan, and Korea, BE was shown to have an IC_{50} value of 88.8 μM

against porcine pancreatic elastase (PPE), comparable to the positive control ursolic acid (IC_{50} = 62.4 μM). BA has also been shown to inhibit elastase, with IC_{50} value of 47.3 μM against PPE in a study of compounds extracted from *Callistemon lanceolatus,* a species of bottlebrush [97]. Interestingly, in a study by Royer et al. (2013) of hot water and ethanol extracts of six Canadian forest species, the ethanolic extract of yellow birch (*B. alleghaniensis)* was the only extract able to completely inhibit elastase (IC_{50} = 0.7 mg/mL), outperforming the positive control Oligopin® (IC_{50} = 1.0 mg/mL), a commercial standardized pine bark extract used in cosmetics and natural health products [34], [98]. The anti-melanogenic effects have also been well-studied in triterpenes, represented by their ability to inhibit tyrosinase, the key enzyme involved in melanogenesis. In a study of compounds extracted from chaga mushroom (*Inonotus obliquus),* a fungus that grows on trunks of birch species, BE was shown to inhibit cellular tyrosinase in B16 melanoma cells more effectively than the positive control kojic acid with IC_{50} values of 5.13 μM and 6.43 μM, respectively. BA extracted from *Rhododendron collettianum* (Ericaceae) has also been reported to be a strong inhibitor of tyrosinase activity, with an IC_{50} value of 2.14 μM against mushroom tyrosinase, which also was significantly more effective than the positive control kojic acid (IC_{50} = 16.67 μM) [99].

1.9 - Transdermal Drug Delivery

The skin is the largest and most accessible organ of the human body, and thus provides a promising route for drug administration. Transdermal drug delivery offers several advantages over oral and intravenous routes of administration, including the avoidance of first-pass metabolism by the liver, controlled delivery, reduced dosing frequency, it is non-invasive, and can be self-administered [100], [101]. The main barrier to transdermal drug delivery is the outermost layer of the skin, the stratum corneum, which limits bioavailability and prevents the penetration of many drugs to the deeper layers of the skin where they are needed [102]. In order to combat this natural skin barrier, special carriers are

required to transport drugs through the skin. One approach for improving skin penetration is the use of vesicular delivery systems such as liposomes and ethosomes.

1.10 - Liposomes

Liposomes are the most investigated nanocarrier for targeted drug delivery, and have been employed to improve a wide array of biomedical therapies by stabilizing compounds, overcoming obstacles involved with cellular uptake, and improving biodistribution of compounds [103]–[105]. They are spherical vesicles that consist of phospholipid bilayers arranged in one or multiple concentric layers around an aqueous core (Figure 2). As a result of their structure, liposomes are able to entrap hydrophilic drugs in their aqueous core and hydrophobic drugs in their bilayer membrane. Because of their composition, liposomes are biocompatible and biodegradable, and are considered to be, for the most part, pharmacologically inactive with low intrinsic toxicity [104]. They facilitate the passage of drugs through biological barriers and cellular membranes by either fusing with membranes and releasing their contents, or being taken up directly by the cell through the process of endocytosis [106]. Although many reports in the past focused on enhancing percutaneous delivery through the use of liposomes, it is now generally agreed that they are of little to no value as carriers for transdermal drug delivery because they are not able to penetrate into the deeper layers of the skin, and remain confined in the stratum corneum [107].

1.11 – Ethosomes for Transdermal Drug Delivery

Ethosomes (Figure 2) are a variation of the well-established drug carrier liposomes, differing mainly in that they contain relatively high concentrations of ethanol (10-50% v/v) in addition to phospholipids and water [108]. They were first described in 1997 by Touitou et al. [109], and since then have been used more and more in the scientific and pharmaceutical fields. Ethosomes range in size from tens of nanometers (nm) to a few micrometers (μm), and have been reported to improve the skin delivery of several drugs [1], [110]. The high concentration of ethanol is what makes ethosomes unique and gives them their enhanced penetration properties. Ethanol is a known penetration enhancer, which acts by

disturbing the skin lipid bilayer organization [111]. Additionally, inclusion of ethanol in the vesicular membrane results in a less densely packed membrane, allowing for more malleable and deformable vesicles compared to conventional vesicles such as liposomes.

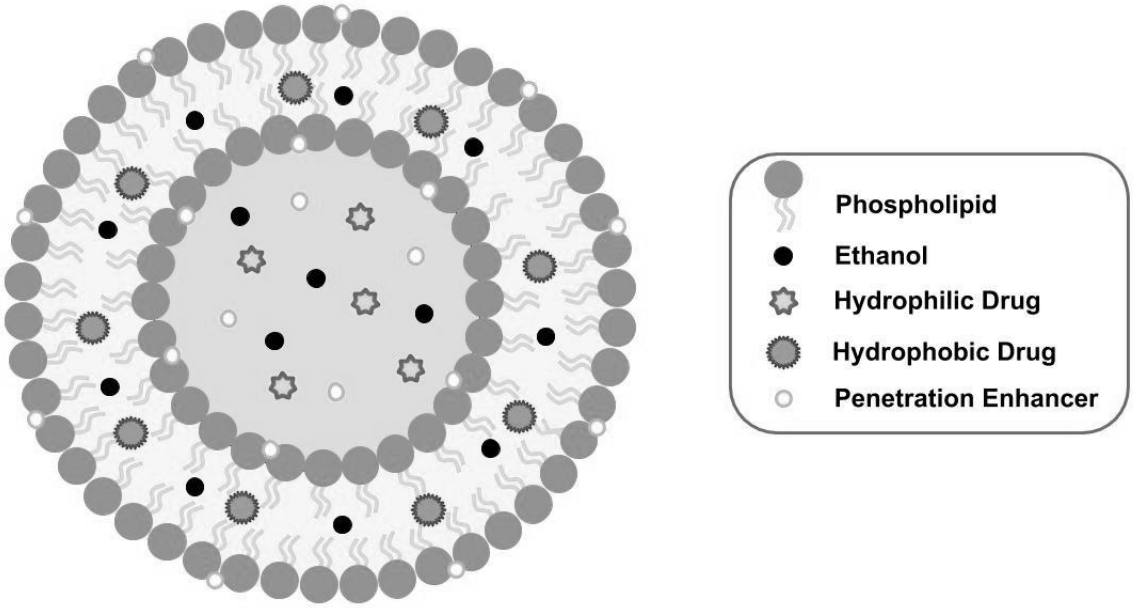

Figure 2: Schematic representation of an ethosome.

1.11.1 - Mechanism of Ethosomal Drug Delivery

Touitou et al. suggested a synergistic mechanism between ethanol, the vesicles, and the lipids of the skin [108]. It is proposed that the first part of the mechanism is due to the ethanol effect, in which the ethanol intercalates with the polar head group environment and increases the permeability of the stratum corneum, effectively increasing its fluidity and decreasing its density. This is followed by the ethosome effect, which involves the penetration of the lipid through the opening of new pathways as a result of the malleability and fusion of ethosomes with skin lipids, allowing for release of drugs into deep layers of skin. This mechanism was later confirmed in a study of the dermal and intracellular deliver of ethosomes containing bacitracin, a polypeptide antibiotic [112].

In a similar study by the same author, three different fluorescent probes were incorporated into ethosomes, hydroethanolic solutions, and liposomes, and the intracellular presence of the probes was detected by confocal laser scanning microscopy (CLSM) and fluorescence-activated cell sorting (FACS) following treatment on mice fibroblasts [113]. CLSM micrographs showed that ethosomes facilitated the penetration of all three probes into the cells as evident from the presence of high-intensity fluorescence. When incorporated into hydroethanolic solution or liposomes, almost no fluorescence was detected.

1.11.2 – Effects of Constituents

There are several components which have been used in ethosomal systems, and while ethanol and a phospholipid are present in all ethosome formulations, several other optional components, such as cholesterol and penetration enhancers like Tweens and Spans are often included in formulations to achieve specific vesicular properties. Ethanol, as mentioned, is a penetration enhancer, and has been reported to effect the size, stability, entrapment efficiency, and skin permeability of ethosomes, and is usually found in concentrations ranging from 10-50% [108], [114]. It is generally agreed that as ethanol concentration increases, the size of vesicles decreases [107], [115]. However, increasing ethanol concentration above optimum levels will lead to a poor entrapment efficiency due to a leaky bilayer and further increment of ethanol concentration will lead to solubilization of vesicles. Reports have suggested that the reduced size of ethosomes due to the presence of ethanol is a result of interpenetration of the ethanol hydrocarbon chain in the vesicular bilayer, leading to reduced membrane thickness, while other studies have suggested the modified net charge that ethanol confers to the vesicles provides some degree of steric stabilization, leading to decreased vesicle size [112], [115]. Phospholipids are one of the main components of ethosomal systems, and based on the type and concentration used, will influence the size, entrapment efficiency, stability, and penetration properties of the vesicular system. Several types and brands of natural and synthetic phospholipids have been employed in ethosome formulations, including dipalmitoylphosphatidylcholine (DPPC) [6], dipalmitoylphosphatidylglycerol (DPPG) [116], L-α-phosphatidylcholine from soybean or egg yolk (PC) [117], Phospholipon 90G [118], Lipoid S100 [119],

Lipoid E80 [120], and others. Generally, phospholipid concentrations ranging from 0.5%-5% are used in ethosome formulations, with vesicular size generally increasing in relation to increasing phospholipid concentration [114], [117]. Increasing the phospholipid concentration will also increase the entrapment efficiency of the formulation to a certain a point, after which further increment in phospholipid concentration will have no effect. Cholesterol is a rigid steroid molecule which is naturally present in biological membranes and is commonly included in the formulation of liposomes and ethosomes. Its incorporation into ethosomal formulations has been reported to increase stability and entrapment efficiency by preventing membrane leakage and reducing vesicular permeability [100]. In addition, it has been reported to increase vesicular size of ethosomes in some cases, as well as increase rigidity [107].

The inclusion of edge activators and penetration enhancers has been widely employed in the preparation of ethosomes to enhance penetration and stability of formulations. Penetration enhancers include oleic acid, dimethyl sulfoxide (DMSO), and L-menthol, which have been reported to influence vesicular size and elasticity as well as increase skin permeation by acting on the stratum corneum [121], [122]. Edge activators are typically surfactants, and include sodium dodecyl sulfate (SDS), polyethylene glycol (PEG), as well as Tweens and Spans and their corresponding grades (80, 60, 40 and 20). Tween-80 is a non-ionic surfactant and is one of the most commonly used edge activators in ethosomal and liposomal formulations. It is typically used in concentrations of 10-50% of the total phospholipid concentration, and has been reported to reduce vesicular size and improve the stability and skin-permeation properties of ethosomal systems [117], [121], [123]. These effects are attributed to Tween-80's solubilizing properties which prevent vesicle fusion and increase the flexibility of the vesicles. It is worth noting that ethosomes containing an edge activator or penetration enhancer are often referred to in literature as "transethosomes", first reported by Song et al. in 2012 in an attempt to combine advantages of classic ethosomes and deformable liposomes (transferosomes) [121]. However, there is still no clear distinction between classic ethosomes and the newer generations and the nomenclature is often used interchangeably.

1.11.3 - Clinical Applications

Ethosomes have been used to enhance the therapeutic effect of a variety of compounds with promising results. Although the majority of published studies examine ethosomes in their initial suspension form, the systems usually need to be incorporated into a suitable vehicle for dermal or transdermal delivery due to the high concentration of alcohol and poor adhesive properties of ethosome solutions. The incorporation into a secondary vehicle for transdermal drug delivery prevents ethanol evaporation, prolongs contact time with the skin, and improves stability of the system and patient compliance. Ethosomes have recently been incorporated into gels [124], [125], transdermal patches [126], [127], and creams [128]. Gels are by far the most common vehicle for the delivery of ethosomes and are produced by incorporating a gel-forming agent such as Carbopol or hydroxypropyl methylcellulose. These polymers, along with their related grades (Carbopol 934, Carbopol 940, Carbopol 974, etc.) are compatible with ethosomal systems and provide the necessary mechanical properties in terms of viscosity and bio-adhesion. Yu et al. recently incorporated mitoxantrone (MTO) into an ethosome gel using hydroxypropyl methylcellulose as a gel forming agent and evaluated its cytotoxicity towards B16 melanoma cells [1]. The ethosome gel outperformed hydroethanolic solutions of MTO in terms of both transdermal permeation and anti-cancer effect.

Ethosomes have also recently been used to improve the skin-lightening effect of phenylethyl resorcinol (PR), a phenolic compound with tyrosinase inhibition activity. Limsuwan et al. (2017) incorporated PR into ethosomes and evaluated the effect on cellular tyrosinase activity in B16 melanoma cells and pig skin compared to PR delivered in liposomes, 20% propylene glycol solutions, and 30% hydroethanolic solutions [8]. Ethosomes consistently exhibited higher tyrosinase inhibition when compared to other formulations in both the B16 melanoma cells and the pig skin. These findings demonstrate that ethosomes are capable of delivering therapeutic agents into the skin efficiently and have great potential for topical applications of anti-melanoma and skin-lightening agents.

Objectives

I: Incorporate birch bark triterpenes into ethosomes and characterize ethosomes based on their size and entrapment efficiency. Ethosomal formulations containing BE, BA, and TE will be prepared based on an optimized formulation. Vesicle size of ethosomes will be measured using diffraction laser particle size analysis, entrapment efficiency will be determined using centrifugation method with high pressure liquid chromatography (HPLC), and the morphology and structure of ethosomes will be determined by visualizing the ethosomes using scanning electron microscopy (SEM).

II: Evaluate the anti-melanoma effect of ethosomal triterpenes on B16-F10 cells. Viability of B16-F10 cells treated with ethosomal triterpenes (E-BE, E-BA, E-TE) will be evaluated by MTT assay and compared to cells treated with free form triterpenes (BE, BA, TE) in ethanolic solutions.

III: Evaluate the anti-melanogenic effect of ethosomal triterpenes in B16-F10 cells. The cellular tyrosinase activity of B16-F10 cells treated with ethosomal triterpenes (E-BE, E-BA, E-TE) will be measured by monitoring the treated cells' ability to convert L-DOPA to dopaquinone and compared with that of free form triterpenes (BE, BA, TE) in ethanolic solutions.

.

2 - Materials and Methods

2.1 - Materials

Cholesterol, Tween-80, Triton X-100, Dulbecco's modified Eagle's medium (DMEM), 3-(4,5-dimethylthiazol-2-yl)-2,5-diphenyltetrazolium bromide (MTT), 3,4-dihydroxy-L-phenylalanine (L-DOPA), 3-isobutyl-1-methylxanthine (IBMX), and kojic acid were obtained from Sigma-Aldrich (St. Louis, MO, USA). Dipalmitoyl phosphatidylcholine (DPPC) was obtained from Transferra Nanosciences (Burnaby, BC, Canada). HyClone fetal bovine serum (FBS) was obtained from Fisher Scientific (Hampton, NH, USA). Betulin (BE), betulinic acid (BA), and The Actives Factory Triterpene Extract (TE) were supplied by The Actives Factory (Hopkins, MN, USA). B16-F10 murine melanoma cell line (CRL-6475) was obtained from the American Type Culture Collection (ATCC, Manassas, VA, USA).

2.2 - Preparation of Ethosomes Containing Triterpenes

Ethosomes were prepared using the Cold Method with slight modification [6]. The lipid phase consisted of appropriate amount of drug (20 mg), 0.2-0.4% w/v DPPC, 1.29 mM cholesterol, and 1 µL/mL Tween-80 dissolved in 100% ethanol (3-5 mL) maintained at 30 °C under magnetic stirring at 1200 RPM in a well-sealed glass bottle. Into this solution, the aqueous phase consisting of 0.01 M phosphate buffered saline (pH 7.4) maintained at 30°C in a separate vessel was added drop-wise with the help of a syringe. The mixture was stirred for an additional 10 minutes following the addition of aqueous phase and allowed to cool to room temperature. The mixture was then sonicated (20 W) for 15 minutes using a digital probe sonicator (Branson Ultrasonics Corporation, Danbury, CT, USA). Temperature of mixture was maintained at approximately 20 °C throughout sonication using a water bath. To remove undissolved components, solutions were filtered through 10 µm nylon filters (Micron Separations Inc., Westborough, MA, USA). The ethosomes produced were stored at 4°C until use. All formulations were

prepared in triplicate (n = 3). For optimization study, betulin was used as the model drug in all formulations. In Table 1, the composition corresponding to all formulations have been reported.

Table 3: Composition of ethosome formulations used in optimization study. Ethosomes were prepared by Cold Method and contained 1.29 mM cholesterol, 4.52 mM betulin, and 1 µL/mL Tween-80.

Formulation	DPPC (% w/v)	Ethanol (% v/v)	0.01 M PBS (% v/v)
A	0.2	30	70
B	0.2	40	60
C	0.2	50	50
D	0.3	30	70
E	0.3	40	60
F	0.3	50	50
G	0.4	30	70
H	0.4	40	60
I	0.4	50	50

2.3 - Characterization of Ethosomes Containing Triterpenes:

2.3.1 - Determination of Vesicle Size of Ethosomes:

Vesicle size was determined by laser diffraction using a Microtrac S3500 Particle Size Analyzer (Microtrac, Largo FL, USA). The average of three measurements was taken for triplicate batches of each formulation. Volumetric distributions were used for calculation of mean particle size. All measurements are presented as mean ± standard deviation (n = 3). Vesicle sizes are reported as the mean value of a volumetric distribution of the data.

2.3.2 - Determination of Entrapment Efficiency of Ethosomes:

The entrapment efficiency (EE) of each ethosome formulation was determined by centrifugation method. The formulations were centrifuged at 16,000 RCF for 1 hour at 4 °C using a Sorvall Legend Micro 17R Centrifuge (Thermo Fisher Scientific, Waltham, MA, USA), after which supernatant was

collected and diluted with 100% ethanol. The amount of drug contained in the diluted supernatant was determined by HPLC. The entrapment efficiency was calculated from the following equation:

$$EE\% = \frac{Qt-Qs}{Qt} \text{ x } 100$$

Where Q_t = the amount of drug added and Q_s = amount of drug detected in supernatant. All measurements are presented as mean ± standard deviation (n ≥ 3).

2.3.3 - Determination of Triterpene Content using High Performance Liquid Chromatography (HPLC):

Betulin, betulinic acid, and The Actives Factory Triterpene Extract were analyzed by Agilent 1260 Series HPLC at 25 °C with a Poroshell 120 EC-C18 2.7 µm column (4.6 x 100 mm) (Agilent Technologies, Santa Clara, CA, USA). The flow rate was 1.0 mL/min with the mobile phase consisting of acetonitrile and water at a ratio of 86:14 (v/v). The column eluent was monitored with a UV detector at 200 nm.

2.3.4 - Visualization of Ethosomes with Scanning Electron Microscopy (SEM):

For visualization by SEM, ethosome formulations were diluted 1:50 with 40% ethanol in 0.01 M PBS and filtered through 0.45 µm PTFE filters, after which 10.0 µL of the diluted vesicular system was homogenously spread onto a glass stub and left to dry overnight at room temperature. The following day, samples were carbon coated using an Edwards Auto 306 carbon coater (Edwards, Crawley, UK) (Lakehead University Instrumentation Lab) and observed under a Hitachi SU-70 Schottky FE-SEM at an accelerating voltage of 10.0 kV (Hitachi, Chiyoda, Tokyo, Japan) (Lakehead University Instrumentation Lab).

2.4 - Cell Culture

B16-F10 murine melanoma cells (American Type Culture Collection # CRL-6475) were maintained in Costar 0.2 μm vent cap culture flasks (Corning, Corning, NY, USA) with standard Dulbecco's modified Eagle's medium (Sigma-Aldrich) supplemented with 10% heat inactivated fetal bovine serum (HyClone Laboratories, Logan, UT, USA) and 1% penicillin/streptomycin (100 U/mL and 100 μg/mL). Cultures were incubated at 37 °C in a humidified atmosphere containing 5% CO_2 until approximately 90% confluence. Cells were subcultured every 48 hours by trypsinization.

2.5 – Preparation of Ethosomal and Ethanolic Triterpene Solutions for Cell Treatment

Prior to cell treatment, ethosomal formulations were filtered through 0.8 μm nylon syringe filters and drug content was re-measured with HPLC to determine final triterpene concentration of filtered solutions. From these, stock solutions of 3 mM were made for each ethosome formulation (BE-ethosomes, BA-ethosomes, TE-ethosomes), and diluted with DMEM to form specific treatment concentrations (0.1 μM, 1 μM, 10 μM, 20 μM). Blank ethosomes were diluted to the same extent to serve as solvent controls for cell treatment. For ethanolic solutions, triterpenes (BE, BA, TE) were dissolved in 100% ethanol to form stock solutions of 10 mM, which were then diluted with DMEM to form specific treatment concentrations (0.1 μM, 1 μM, 10 μM, 20 μM). Final ethanol concentration in cell treatments did not exceed 0.25%.

2.6 - Measurement of Cell Viability

Cell viability was determined using MTT assay, in which mitochondrial and cytosolic dehydrogenases of viable cells reduce yellow MTT (3-(4,5-dimethylthiazol-2-yl)-2,5-diphenyltetrazolium bromide) to purple formazan that can be measured spectrophotometrically [129]. B16-F10 murine melanoma cells were seeded at 1.0 x 10^4 cells/well into sterile 96-well flat-bottom plates (Corning) for 24

hours, then incubated with test substances for 48 hours at 37°C in a humidified atmosphere containing 5% CO_2. During final 4 hours of treatment, 20 µL of MTT solution (5 mg/mL dissolved in PBS) was added to each well. Following treatment, media was removed and 150 µL of dimethyl sulfoxide (DMSO) was added to solubilize formazan crystals. After gentle shaking for 10 minutes, absorbance was measured spectrophotometrically at 570 nm using PowerWave XS Microplate Spectrophotometer (BioTek, Winooski, VT, USA). The viability of treated wells was compared to that of control wells, which were taken to have 100% viability.

2.7 - Measurement of Cellular Tyrosinase Activity

Cellular tyrosinase activity was determined by the method described by Tomita et. al with some modification [130]. B16-F10 murine melanoma cells were seeded at 1.0 x 10^4 cells/well into sterile 96-well flat-bottom plates (Corning) for 24 hours. Following incubation with test substances in the presence of 100 µM 3-isobutyl-1-methylxanthine (IBMX) for 48 hours, cells were washed with ice-cold PBS and lysed with PBS containing 1% Triton-X (80 µL/well), then frozen at -80°C for 30 minutes. After thawing and mixing, 20 µL of 10 mM L-DOPA was added to each well, and cells were incubated for 2 hours at 37°C, after which absorbance was measured at 490 nm using PowerWave XS Microplate Spectrophotometer (BioTek). The relative activity of treated wells was compared to that of control wells, which were taken to have 100% activity.

3 - Results

3.1 - Optimization of Ethanol and DPPC Concentration in Ethosome Formulations

Initially, an optimization study was carried out to determine the most suitable phospholipid and ethanol concentration for the ethosomal system. Ethosome formulations containing 0.2-0.4% w/v DPPC and 30-50% v/v ethanol were prepared as described and characterized based on their mean vesicle size and entrapment efficiency (Table 4). Betulin was used as the model drug for all nine formulations. Ranges of phospholipid and ethanol content were selected based on preliminary work not shown, in which it was determined the inclusion of DPPC at concentrations greater than 0.5% w/v resulted in the formation of a colloidal gel upon sonication, whereas concentrations below 0.2% resulted in vesicles inconsistent in size and morphology. The inclusion of <30% v/v of ethanol was insufficient to solubilize components of the lipid phase, whereas inclusion >50% v/v ethanol resulted in disruption of the lipid vesicles. Ethosome formulations in the optimization study ranged in mean vesicle size from 3.67-15.08 μm, with entrapment efficiencies ranging from 88.67-98.68%. With the exception of formulation F, the mean vesicle size decreased in relation to increasing ethanol concentration. Entrapment efficiency increased in relation to increasing ethanol concentration with the exception of formulations containing 0.2 % w/v DPPC (A-C), in which the opposite trend was observed. When DPPC concentration was increased from 0.2 % w/v to 0.3 % w/v, the mean vesicle size of formulations decreased, but increased when the DPPC concentration was further increased to 0.4 % w/v. For formulations containing 30% and 40% ethanol, the entrapment efficiency decreased with increasing DPPC concentration, but the opposite trend was observed for formulations containing 50% ethanol, in which entrapment efficiency increased in relation to increasing DPPC concentration. Based on the desired characteristics of a stable vesicle formulation with a size of ≤5 μm and an entrapment efficiency greater than 90%, formulation E (0.3% w/v DPPC, 40% v/v ethanol) was chosen for all further vesicle preparations which was determined to have a mean vesicle size of 3.67 μm and an entrapment efficiency of 95.76%.

3.2 - Formulation and Characterization of Ethosomes Containing BE, BA, and TE

Using formulation E from the optimization study (0.3% w/v DPPC, 40% v/v ethanol), ethosomes containing betulin (BE), betulinic acid (BA) and The Actives Factory Triterpene Extract (TE) were prepared and characterized in terms of mean vesicle size and entrapment efficiency (Table 5). A blank ethosome (no drug content) was also prepared for comparative purposes. The mean vesicle sizes of ethosomes containing BE, BA, and TE ranged from 2.57–5.11 μm, while the entrapment efficiencies ranged from 93.25-95.76%. The blank ethosome was determined to have a mean vesicle size of 3.79 μm.

To determine the structure and surface morphology of BE-ethosomes, BA-ethosomes, and TE-ethosomes, formulations were diluted 50:1, filtered through 0.45 μm PTFE filters, and observed using SEM (Figure 2-5). For all ethosomal systems, the presence of larger vesicles ranging from 200-500 nm (Figure 2-5-A) distributed among smaller, uniformly-sized ethosomes approximately 50 nm in size (Figure 2-5-B) was observed. The ethosomes were mainly spherical in shape, with increasing irregularity in shape present among the larger vesicles. The smaller vesicles showed much higher uniformity in terms of shape and size.

Table 4: Vesicle size and entrapment efficiency of ethosomes produced in optimization study. Ethosomes were prepared containing 2 mg/mL (4.52 mM) betulin, 1.29 mM cholesterol, 1.0 μL/mL Tween-80, and 0.01 M PBS up to 100% v/v.

Formulation	DPPC (%w/v)	Ethanol (% v/v)	Vesicle Size (μm)	Entrapment Efficiency (%)
A	0.2	30	10.21 ± 3.63	98.40 ± 0.28
B	0.2	40	8.49 ± 1.45	96.33 ± 0.73
C	0.2	50	8.27 ± 1.76	93.97 ± 7.74
D	0.3	30	6.67 ± 2.54	91.25 ± 1.34
E	**0.3**	**40**	**3.67 ± 0.10**	**95.76 ± 0.85**
F	0.3	50	4.22 ± 0.84	97.66 ± 0.72
G	0.4	30	15.08 ± 2.07	88.67 ± 4.15
H	0.4	40	11.00 ± 1.40	93.65 ± 4.34
I	0.4	50	6.67 ± 1.30	98.68 ± 0.68

Each data represents the mean ± SD (n=3)

Table 5: Vesicle size and entrapment efficiency of ethosomes containing birch bark triterpenes. Ethosomes were prepared with 1.29 mM cholesterol, 1.0 µL/mL Tween-80, and 0.01 M PBS up to 100% v/v and 2 mg/mL of either BE (4.52 mM), BA (4.38 mM), or TE.

Compound	DPPC (% w/v)	Ethanol (% v/v)	Vesicle Size (µm)	Entrapment Efficiency (%)
E-BE	0.3	40	3.67 ± 0.78	95.76 ± 0.85
E-BA	0.3	40	5.11 ± 0.52	93.33 ± 0.73
E-TE	0.3	40	2.57 ± 0.33	93.25 ± 1.34
Blank	0.3	40	3.79 ± 0.41	-

Each data represents the mean ± SD (n=3)

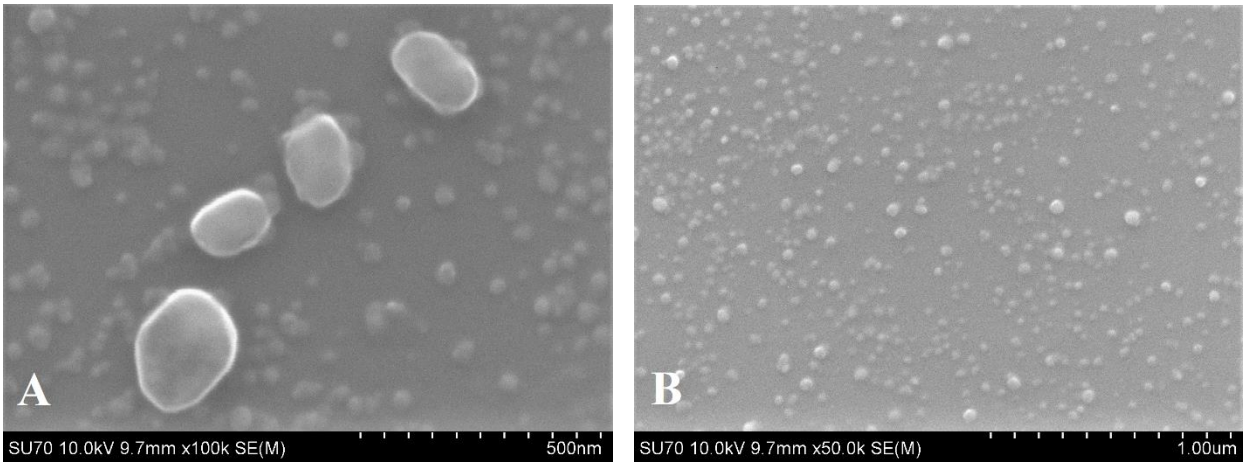

Figure 3: **Scanning electron micrographs of BE-ethosomes.** BE-ethosomes were carbon coated and visualized with SEM at A) 100,000 X and B) 50,000 X.

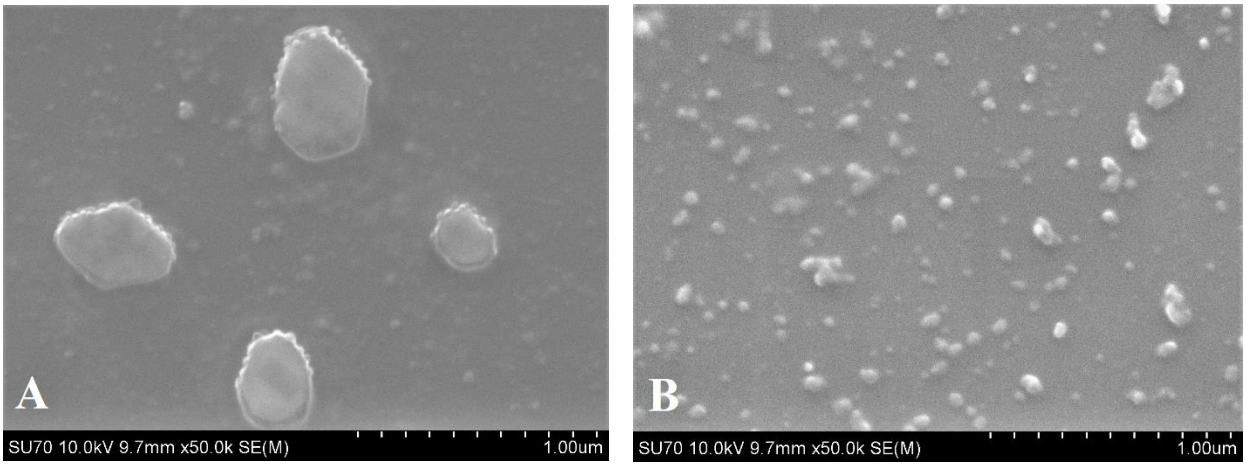

Figure 4: **Scanning electron micrographs of BA-ethosomes.** BA-ethosomes were carbon coated and visualized with SEM at 50,000 X.

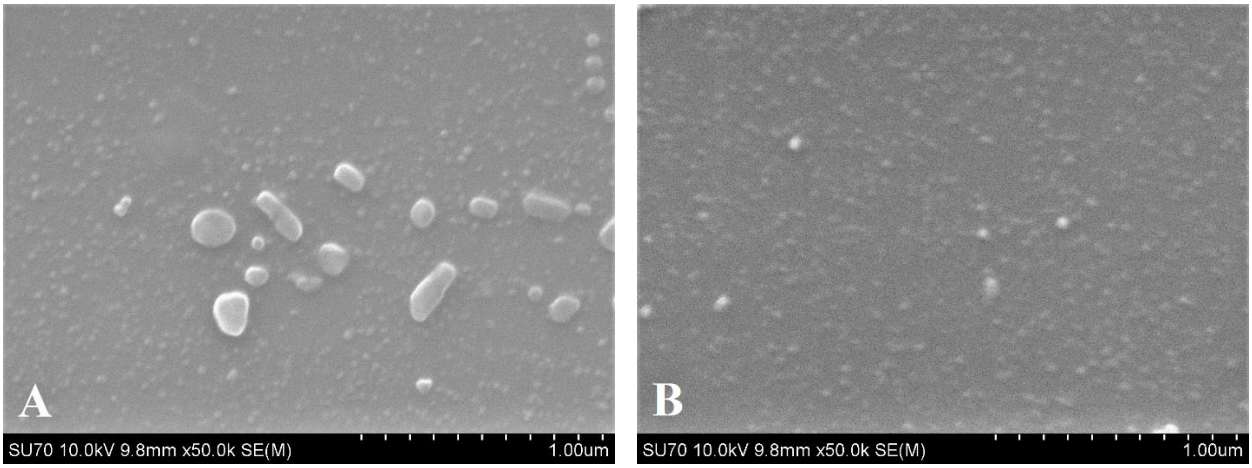

Figure 5: **Scanning electron micrographs of TE-ethosomes.** TE-ethosomes were carbon coated and visualized with SEM at 50,000 X.

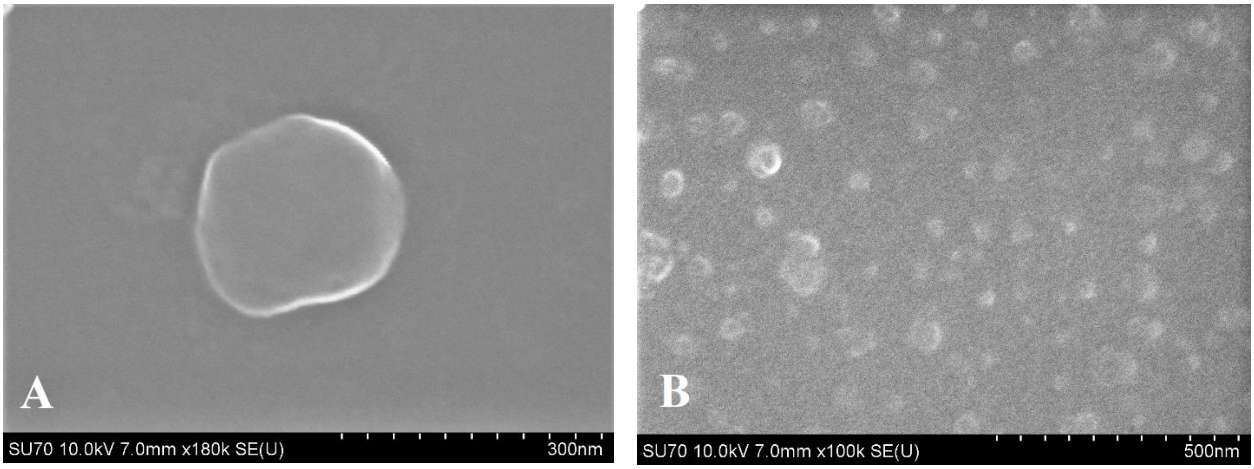

Figure 6: Scanning electron micrograph of blank ethosome. Blank ethosomes were carbon coated and visualized with SEM at A) 180,000 X, and B) 100,000 X.

3.3 - Effect of E-BE and BE on Viability of B16-F10 Melanoma Cells

To assess the effects of BE, BA, and TE on B16-F10 melanoma cells, cells were treated with increasing concentrations of the triterpenes delivered in both ethosomes as well as their free form in ethanolic solutions (0.1, 1, 10, 20 μM) for 48 hours. For both E-BE and BE, the viability of B16-F10 melanoma cells decreased in a concentration-dependent manner relative to control cells as determined by

the MTT colourimetric assay (Figure 7). A moderate effect on cell viability was observed even at the lowest concentration (0.1 μM), with ~30% cell death in cells treated with E-BE, and ~15% cell death in cells treated with BE. The relative viability of cells treated with E-BE was lower for all concentrations, with 40.57% relative viability at 1 μM, 30.14% at 10 μM, and 29.74% at 20 μM, compared to 65.57%, 57.47%, and 40.47%, respectively, at the same concentrations when delivered in ethanolic solutions.

3.4 - Effect of E-BA and BA on Viability of B16-F10 Melanoma Cells

In B16-F10 cells treated with BA, a similar effect was observed as with BE. E-BA and BA both induced a concentration-dependent reduction in relative cell viability (Figure 8). For E-BA at concentrations of 0.1, 1, 10, and 20 μM, the relative viability of cells was 76.67%, 37.00%, 26.54% and 29.58%, compared to 88.59%, 69.80%, 59.39%, and 44.98%, respectively, in ethanolic solutions of BA. Of all treatments, 10 μM E-BA was the most effective.

3.5 - Effect of E-TE and TE on Viability of B16-F10 Melanoma Cells

For ease of comparison, all TE concentrations are presented in μM units assuming the same molecular weight as BE (442.72 g/mol) since the triterpene extract is composed mainly of BE, with most other components having similar molecular weights. The actual concentrations corresponding to 0.1, 1, 10, and 20 μM are 0.23 μg/mL, 2.23 μg/mL, 22.6 μg/mL, and 45.2 μg/mL, respectively. TE showed the least toxicity towards B16-F10 cells among all treatments. E-TE and TE induced concentration-dependent reduction of cell viability (Figure 9), with the highest cytotoxicity observed in TE at a concentration of 20 μM, in which the relative cell viability was determined to be 37.69% in comparison to 52.48% with 20 μM E-TE. This was the only concentration among all drug treatments in which the ethanolic solution out-performed the ethosomal solution of the same concentration. The relative cell viability at E-TE concentrations of 0.1, 1, and 10 μM were 79.60%, 60.35%, and 55.82%, respectively. In comparison, the relative cell viabilities for TE at the same concentrations were 89.70%, 73.76%, and 70.64%, respectively. The IC_{50} values, which represent the concentration of drug at which cell growth was

inhibited by 50%, were determined for all treatments based on individual dose-response curves (Table 6). The IC_{50} value was lower for E-BE and E-BA compared to ethanolic solutions of BE and BA, indicating an improvement in cytotoxic effect as a result of incorporation into the ethosomal system. The IC_{50} value for E-TE was higher than for ethanolic solutions of TE, suggesting that no improvement in cytotoxicity was provided by incorporation into the ethosome.

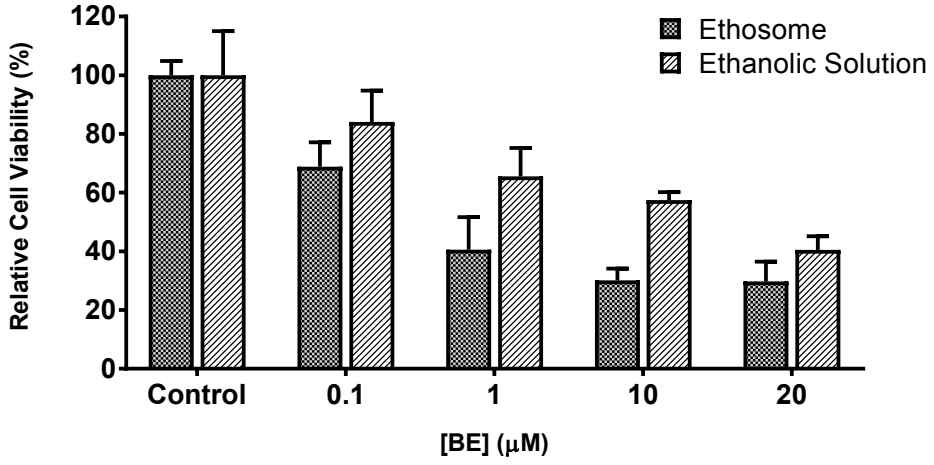

Figure 7: Effect of E-BE and BE on cell viability of B16-F10 cells. Viability of cells treated with ethanolic-BE and ethosomal-BE was determined by measuring the activity of mitochondrial dehydrogenases using MTT colourimetric assay. B16-F10 melanoma cells seeded in 96-well plates at a density of 10,000 cells/well were treated with increasing concentrations of BE formulations for 48 hours and incubated with MTT reagent during the final 4 hours of treatment after which absorbance was measured at 570 nm. Cell viability was assessed relative to control cells. Each data represents the mean ± SD (n=3).

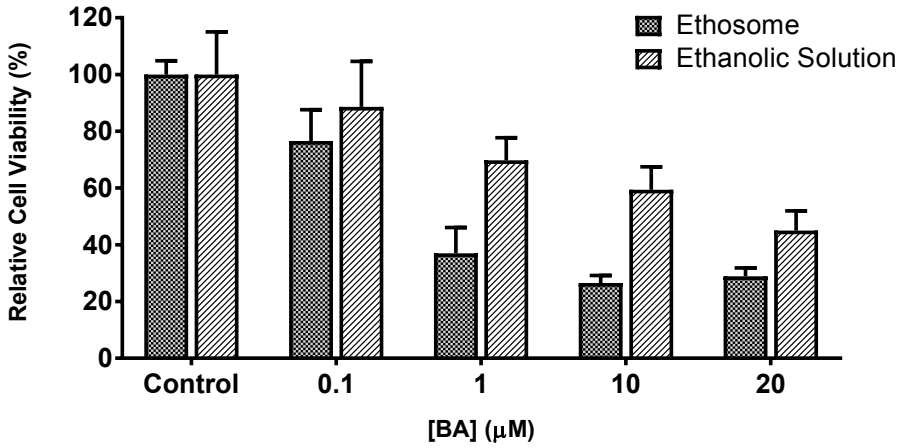

Figure 8: Effect of E-BA and BA on cell viability of B16-F10 cells. Viability of cells treated with ethanolic-BA and ethosomal-BA was determined by measuring the activity of mitochondrial dehydrogenases using MTT colourimetric assay. B16-F10 melanoma cells seeded in 96-well plates at a density of 10,000 cells/well were treated with increasing concentrations of BE formulations for 48 hours and incubated with MTT reagent during the final 4 hours of treatment after which absorbance was measured at 570 nm. Cell viability was assessed relative to control cells. Each data represents the mean ± SD (n=3).

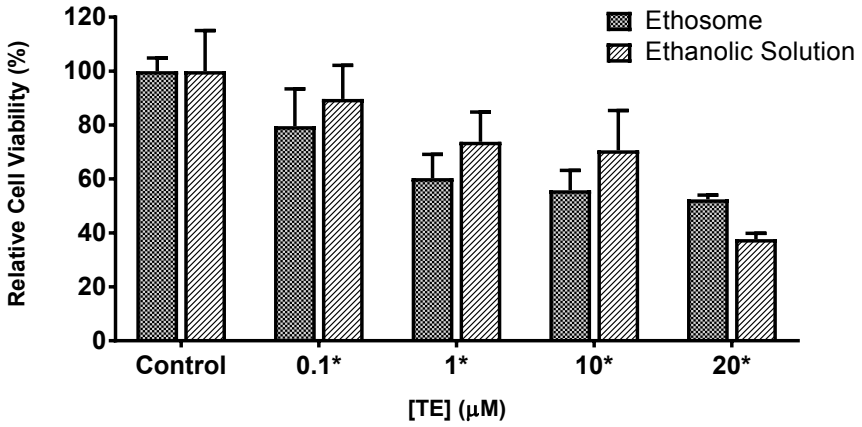

Figure 9: Effect of E-TE and TE on cell viability of B16-F10 cells. Viability of cells treated with ethanolic-TE and ethosomal-TE was determined by measuring the activity of mitochondrial dehydrogenases using MTT colourimetric assay. B16-F10 melanoma cells seeded in 96-well plates at a density of 10,000 cells/well were treated with increasing concentrations of BE formulations for 48 hours and incubated with MTT reagent during the final 4 hours of treatment after which absorbance was measured at 570 nm. Cell viability was assessed relative to control cells. Each data represents the mean ± SD (n=3). * = concentrations assuming same molecular weight as BE (442.7 g/mol).

Table 6: Cytotoxic effect of birch bark triterpenes on B16-F10 melanoma cells. B16-F10 melanoma cells were treated for 48 hours with BE, BA, or TE delivered in ethosomes or in ethanolic solutions.

Treatment	IC_{50} (μM)	IC_{50} (μg/mL)
BE	14.38	32.50
E-BE	2.43	5.45
BA	16.41	35.90
E-BA	3.07	6.72
TE	-	36.00
E-TE	-	43.51

IC_{50} = concentration of drug at which cell growth was inhibited by 50%

3.6 - Effect of Ethosomal Triterpenes on Cellular Tyrosinase Activity in B16-F10 Melanoma Cells

To investigate the effects of BE, BA, and TE on cellular tyrosinase activity, B16-F10 cells were treated with 10 nM solutions of the triterpenes both in ethosomes and in ethanolic solutions, a concentration at which the compounds would not affect the viability of the cells (Figure 9). All treatments caused a moderate reduction in the relative activity of tyrosinase, and although ethosomal solutions caused more of a reduction in relative activity, there were no significant differences between ethosomal and ethanolic treatments at such low concentrations. Cells treated with 10 nM E-BE showed relative tyrosinase activity of 72.53%, compared to 81.60% when treated with BE. Similarly, 10 nM E-BA showed relative tyrosinase activity of 71.67% compared to 79.23% for BA. Cells treated with 10 nM solutions of TE showed the least effect, with relative tyrosinase activity of 77.97% in E-TE and 83.15% relative activity in TE. For comparison, B16-F10 cells were also treated with kojic acid, a standard tyrosinase inhibitor, at concentrations from 1-500 μM (Figure 10). Kojic acid was found to reduce cellular tyrosinase activity in a concentration-dependent manner. Though it had no effect at 1 and 10 μM, the relative activity of tyrosinase was reduced to 67.63% at 100 μM, 36.25% at 250 μM, and 24.06% at 500 μM.

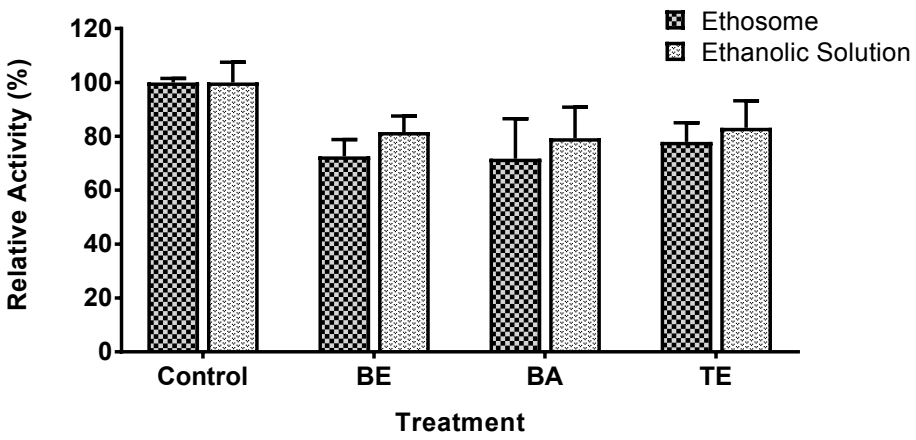

Figure 10: Effects of birch bark triterpenes on cellular tyrosinase activity. B16-F10 cells seeded at 10,000 cells/well in 96-well plates were treated with 10 nM BE, BA, and TE in ethosomes and ethanolic solutions for 48 hours in the presence of 100 μM IBMX. Following treatment, cells were incubated with L-DOPA for 2 hours after which absorbance was measured at 490 nm. Tyrosinase activity was assessed relative to control cells. Each data represents the mean ± SD (n=3).

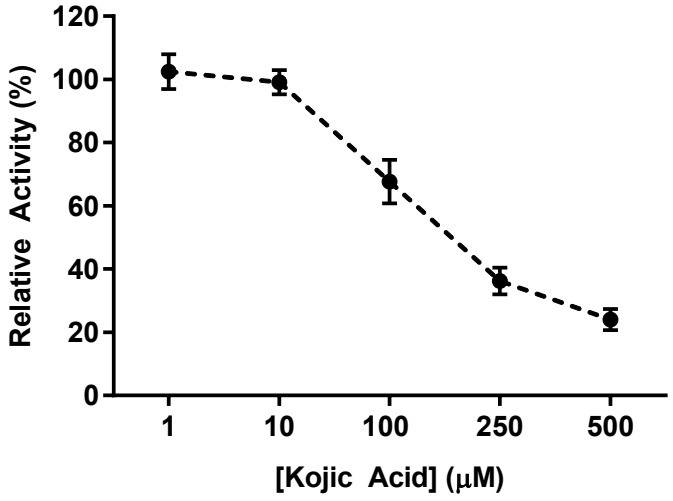

Figure 11: Effect of kojic acid on cellular tyrosinase activity. B16-F10 cells seeded at 10,000 cells/well in 96-well plates were treated with increasing concentrations of kojic acid for 48 hours in the presence of 100 μM IBMX. Following treatment, L-DOPA was added to wells for 2 hours after which absorbance was measured at 490 nm. Tyrosinase activity was assessed relative to control cells. Each data represents the mean ± SD (n=3).

Discussion

Betulin (BE) and betulinic acid (BA) are readily extracted from North American birch species of the boreal forest, and have been reported to show significant cytotoxicity towards human and animal melanoma cell lines [62]–[64]. Despite their promising bioactivity and established low toxicity towards normal cells, their use in pharmaceuticals and cosmetics has traditionally been limited by their poor hydrosolubility. A common strategy that has been employed to overcome poor hydrosolubility of compounds is encapsulating them in a specialized vehicle to improve their hydrosolubility and bioavailability. Ethosomes, an ethanolic variation of the well-established drug carrier liposomes, have recently been used to encapsulate hydrophobic compounds [116], improve transdermal drug delivery [118], as well as improve the anti-melanoma effect and skin-lightening effect of various compounds [1], [44]. Because of their established potential as vehicles for drug delivery, especially in topical applications, ethosomes were investigated as a drug delivery vehicle for BE, BA, as well as a triterpene extract (TE) from the outer bark of *Betula papyrifera*.

The main factors influencing the characteristics of ethosomal formulations in terms of vesicle size and entrapment efficiency are ethanol (EtOH) and phospholipid concentration. In order to determine a suitable formulation for encapsulating BE, BA, and TE in ethosomes, an optimization study was carried out using a range of EtOH and phospholipid (in this case DPPC) concentrations. In total, nine formulations were prepared with combinations of EtOH concentrations of 30%, 40%, and 50% v/v, and DPPC concentrations of 0.2%, 0.3%, and 0.4% w/v. Most commonly, phospholipid concentration in ethosomal formulations ranges from 0.5-5.0%, but is very much dependent on the type of phospholipid used. DPPC has been used in ethosomal formulations at concentrations ranging from 0.1-3.0% w/v [6], [131]. Preliminary work based on the physical appearance of formulations in this study was conducted in which DPPC concentrations of 0.5-1.0% resulted in the formation of a gel-like colloidal suspension upon sonication. Alternatively, concentrations ranging from 0.1-0.2% resulted in formulations that were inconsistent in stability and physical appearance. Therefore, DPPC concentrations ranging from 0.2- 0.4%

were used in the optimization study to investigate the effects of DPPC concentration on vesicle size and entrapment efficiency (Table 3). In the same preliminary work, EtOH concentrations ranging from 20% to 60% v/v were examined. It was observed that concentrations of 20% were incapable of solubilizing all components of the lipid phase (DPPC, cholesterol, BE), while concentrations of 60% appeared to disrupt the lipid vesicles. Thus, EtOH concentrations ranging from 30-50% v/v were used to investigate the effects of EtOH concentration on vesicle size and entrapment efficiency. Using BE as a model drug for encapsulation at a concentration of 2 mg/mL (4.52 mM), nine formulations in total were prepared in triplicate, composed of different combinations of DPPC and EtOH concentrations (Table 3), and characterized based on their mean vesicle size and entrapment efficiency (Table 4). In order to improve stability, cholesterol and Tween-80 were included in ethosomal formulations. Cholesterol, which is known to prevent aggregation of vesicles as well as increase the rigidity of membranes in liposomes and ethosomes [107], was used at a concentration of 0.5 mg/mL (approximately 20% of the total phospholipid concentration). This conferred some stabilizing effect while maintaining the malleability of the lipid bilayer as observed in SEM images (Figure 3-6). Tween-80 was included at a concentration of 1 μL/mL in formulations (approximately 30% of total phospholipid concentration), which provided a sufficient stabilizing effect compared to solutions prepared without Tween-80. It was observed that the inclusion of cholesterol and Tween-80 prolonged the stability of the formulations and prevented separation over time.

The ethosomes produced in the optimization study ranged in size from 3.67 - 15.08 μm, which is larger than most reported sizes for ethosomal systems. However, when employing particle size analysis, it is important to understand how the data reflects the actual sample. Particle sizes distributions can be generated by several models, but are most commonly measured as a number or a volume distribution [132]. Each technique generates a different result because each technique measures different properties of the sample [132]. In the case of a number distribution, each particle has equal weighting towards the distribution regardless of size or volume. With volume distributions, larger particles contribute significantly more towards the distribution because their volume/mass is taken into account. Thus, the

mean of a volume distribution will generally be higher than the mean of a number distribution generated from the same set of data. Particle analyzers that measure samples on the basis of laser diffraction, such as the one used in this study, construct their result as a volume distribution, therefore the sizes reported in this study represent the mean value of a volume distribution. As a result, despite the presence of a majority of smaller particles in the range of 50 nm as determined by SEM (Figures 3-6), the presence of larger particles in the micron range will shift the average towards the largest particles. If data sets were represented as a number distribution, the mean vesicle size of ethosome formulation would likely have been more representative of the smaller particles. However, this is not to say that a large mean vesicle size is unfavourable. Though smaller vesicles may offer advantages in terms of circulation and permeability, larger vesicles can generally incorporate a much higher payload of the active compound. In one of the few studies involving encapsulation of BA in a liposome, Mullauer et al. (2011) found that small liposomes ranging in size from 100-200 nm were capable of incorporating no more than 1 mg/mL [133]. When they produced larger liposomes ranging from 1-1.5 μm, they found that they were able to incorporate up to 6 mg/mL of BA.

In most reported cases, the size of ethosomes increases as the concentration of phospholipid increases [117], however in this study there was no definitive trend observed. On average, the ethosomes prepared with 0.3% DPPC yielded the lowest vesicle sizes (3.67 – 6.67 μm), followed by ethosomes prepared with 0.2% DPPC (8.27 – 10.21 μm), and the largest ethosomes on average were prepared with 0.4% DPPC (6.67 – 15.08 μm). A similar trend was observed in a study by Bodade et al. (2013), in which ethosomes were prepared with 0.1%, 0.2%, and 0.3% DPPC and the smallest vesicle sizes were observed in formulations containing 0.2% DPPC, suggesting that in the lower range of phospholipid concentrations, a linear trend between vesicle size and phospholipid concentration is not always observed [6]. With regards to EtOH, a more predictable effect took place, in which increasing the concentration of EtOH while maintaining DPPC concentration resulted in smaller vesicle sizes in all cases except formulation F (50% EtOH, 0.3% DPPC, 4.22 μm), which was marginally larger than formulation E (40%

EtOH, 0.3% DPPC, 3.67 μm). Again, the same trend was observed by Bodade et al. (2013), in which increasing EtOH concentrations (25%, 35%, 45%) yielded smaller vesicles while the DPPC concentration was maintained at either 0.1%, 0.2%, or 0.3% DPPC [6]. EtOH's ability to reduce vesicular size has been attributed to the EtOH hydrocarbon chain's ability to interpenetrate the vesicular bilayer and reduce membrane thickness, while other reports suggest the reduction in size stems from the modified net charge that ethanol confers which provides some degree of steric stabilization [112], [117]

There are few reports of the encapsulation of BA in liposomal carriers [133]–[137], and even fewer on the encapsulation of BE [138]. There are no studies investigating the biological effects of liposome containing BE, although it has been suggested due to the enhanced anti-tumour effect of BE when delivered in combination with cholesterol [70]. To the best of the author's knowledge, this study represents the first time BE and BA have been incorporated into ethosomes (or transethosome) and is the first investigation of the bioactivity and/or encapsulation of The Actives Factory Triterpene Extract (TE). Using the optimized formulation which contained 0.3% DPPC and 40% EtOH, ethosomes were prepared containing BE, BA, and TE. The triterpenes and phospholipids were incorporated at a molar ratio of approximately 1:1 (50 molar %) in order to attain the highest concentration of triterpenes in the lipid bilayers of the ethosomes. In order to remove any un-entrapped drug, solutions were filtered through 10 μm nylon filters following preparation. Following filtration, >90% of the drug remained in ethosomal solutions (Table 4). The entrapment efficiencies in this study correspond well with a recent report in which Guo et al. (2017) produced folate-functionalized BA-liposomes with an entrapment efficiency of 91.61 % [137]. Prior to cell treatments, ethosomal solutions were further filtered through 0.8 μm nylon filters to remove any larger vesicles, and the drug content of the formulations was re-measured by HPLC. Following the filtration through 0.8 μm membranes, the drug concentration in formulations was still above 80% of the original amount added in all formulations. The re-calculated entrapment efficiency was 94.50% for BE-ethosomes, 88.14% for BA-ethosomes, and 83.64% for TE-ethosomes, with any loss in drug content attributed to the larger ethosomes which were removed by filtration. This suggests that the

vast majority of BE, BA, and TE was entrapped within the smaller vesicles which were not lost during filtration, especially in BE-ethosomes which only lost ~1% of drug content during the filtration step. Former studies reported that DPPC-triterpene liposomes were capable of entrapping only small amounts of triterpene constituents in lipid bilayer (~ 10 molar %) [138], but these results suggest that ethosomes are capable of entrapping triterpenes at much higher molar ratios.

The treatment of B16-F10 melanoma cells with BE, BA, and TE resulted in a concentration-dependent decrease in cell viability as determined by the MTT assay (Figure 7-9), a commonly used method of measuring *in vitro* cytotoxicity [139]. For each compound, cells were treated in the range of 0.1 μM to 20 μM, which was selected based on former reports of the effects on BE and BA on the B16-F10 cell line [63]. Based on dose-response curves for ethosomal and ethanolic solutions of BE, BA, and TE, the IC_{50} values were determined for all treatments, which represents the concentration of the compound that inhibited cell growth by 50% (Table 6). BE and BA both had a significant cytotoxic effect on B16-F10 cells, with IC_{50} values of 14.38 μM and 16.41 μM, respectively, which correspond well with former reports of the compounds' effects on B16-F10 melanoma cells. Gauthier et al. (2006) investigated several lupane type triterpenes including BE and BA and their cytotoxic effects on three cancerous cell lines including B16-F10 [63]. The reported IC_{50} values for BE and BA in their study were 13.8 μM and 16.1 μM, respectively. In that study, the authors attempted to enhance the pharmacological properties of the compounds via the addition of sugar moieties at the C-3 or C-28 position, which resulted in a loss of cytotoxicity for BE but improved the IC_{50} of BA to 3.9 μM in B16-F10 cells. These results confirm BE and BA as potent cytotoxic agents. The cytotoxic effect of TE (IC_{50} = 36.00 μg/mL) was quite similar to that of BE (IC_{50} = 32.50 μg/mL) and BA (IC_{50} = 35.90 μg/mL), which was expected based on its composition which mainly consists of BE (65%), and considerable BA content (7%) (Table 2). The presence of other triterpene compounds in the extract such as lupeol, which accounts for 7% of the extract, may have hindered its cytotoxic effect against B16-F10 cells, as it has been shown to be inactive against both human and mouse melanoma cells lines [63]. The effects of other betulin derivatives in the

extract such as betulin aldehyde (2% content) are less studied on murine melanoma cells, but have been shown to exhibit distinct cytotoxicity towards human melanoma lines G361 and SK-MEL-28 with IC_{50} values of 9.4 μM and 9.3 μM, respectively [62]. Hata et al. (2003) further showed that lupane triterpenes with an aldehyde group at C-17 selectively inhibited leukemia cell growth, and similar to with betulinic acid, the carbonyl group at C-17 is responsible for the inhibitory activities through the inhibition of topoisomerase I, a common target in chemotherapeutic agents. The interference of DNA topoisomerases, which are essential for DNA replication, will interfere with cell cycle and ultimately trigger cell death [140].

When delivered in ethosomes, the cytotoxic effect of BE and BA was improved at all concentrations (Figure 7-8). The IC_{50} value for E-BE was 2.43 μM compared to 14.38 μM when delivered in its free form in ethanolic solutions. The same effect was observed with E-BA (IC_{50} = 3.07 μM), which was more effective at all concentrations compared to BA in its free form in solution (IC_{50} = 16.41 μM). As previously mentioned, no studies to date, to the best of our knowledge, have investigated the effects of BE delivered in liposomes or ethosomes. However, there are several reports investigating BA delivered in liposomes to improve cytotoxic effect, the results of which align well with this study. BA was previously incorporated into liposomes and used to treat mice xenografted with human colon and lung cancer tumours [133]. In that study, BA-liposomes were delivered intravenously and reduced tumour growth by >50% compared with the control treatment (an empty liposome) but were not compared directly to free form BA in solution. More recently, Liu et al. (2016) modified BA-liposomes with PEG-2000, in which PEGylated BA-liposomes were shown to improve the bioavailability of BA, and showed higher cytotoxic effect *in vitro* and *in vivo* over both traditional BA-liposomes and BA in solution [136]. Ethosomes and liposomes have also been used as delivery systems for a variety of botanical extracts, including Aloe vera leaf extract [141], curcumin extract [142], seabuckthorn leaf extract [143], with generally promising results. In this case, the cytotoxic effect of TE was not significantly improved by delivery in ethosomes (Figure 9). Although E-TE showed moderate improvement in cytotoxic effect at 0.1, 1, and 10 μM, TE

was more effective in its free form at a concentration of 20 μM, which resulted in a lower IC_{50} value for TE in ethanolic solutions than E-TE. In the future, cell viability experiments will need to be assessed across a broader range of concentrations to evaluate the cytotoxic effects of TE. The improvement in anti-melanoma effect observed in E-BE and E-BA suggests that the ethosome carriers facilitated increased uptake of the triterpenes into the cells over ethanolic solutions. Larger ethosomal vesicles would likely have fused with cellular membranes and released the triterpene contents into the cell, while smaller ethosomes may have been directly taken up by the cell through endocytosis [106].

Ethosomes have recently been shown to improve the anti-melanogenic properties of compounds. Limsuwan et al. (2017) incorporated phenylethyl resorcinol (PR), a skin-lightening agent, into ethosomes and reported higher tyrosinase inhibition in B16 melanoma cells compared to PR delivered in liposomes and hydroethanolic solutions [8]. Briefly, ethosomal and ethanolic formulations of BE, BA, and TE were assessed for their ability to inhibit cellular tyrosinase in B16-F10 cells (Figure 10) and compared to a standard tyrosinase inhibitor kojic acid (Figure 11). Cells were treated with ethosomal triterpenes and ethanolic triterpenes in the presence of 100 μM 3-isobutyl-1-methylxanthine (IBMX), which is known to induce melanogenesis, leading to increased synthesis of tyrosinase [144]. Following treatment with test substances, L-DOPA was added to the wells and the oxidation of L-DOPA to dopaquinone, the precursor of melanin, was monitored at 490 nm. Because ethosomal triterpenes showed approximately 20-30% cell death at 0.1 μM concentrations, cells were treated with 10 nM solutions of the triterpenes in ethosomes and ethanolic solutions to avoid any significant effect on cell viability. Kojic acid was tested at a range of 1-500 μM because it has been shown to have minimal effect on viability of B16-F10 cells up to 500 μM [145]. At such low concentrations, the effect on cellular tyrosinase of ethosomal and ethanolic triterpenes was only moderate, and there was no distinguishable improvement in effect conferred by the delivery in ethosomes at the selected concentration. Still, ethosomal triterpenes and ethanolic triterpenes at a concentration of 10 nM showed higher inhibition of cellular tyrosinase than the standard inhibitor kojic acid at 1-10 μM, which supports their use cosmetic and skin-lightening applications.

The results from this study are preliminary but indicate that ethosomes are a promising vehicle for improving the effects of triterpenes such as BE, BA, and TE. Ethosomes were shown to successfully encapsulate BE, BA, and TE with high entrapment efficiency. They were also shown to enhance anti-melanoma effect of both BE and BA as demonstrated by their increased cytotoxicity towards B16-F10 melanoma cells. Although there was no significant improvement in the anti-melanogenic effects of the triterpenes when delivered in ethosomes, further studies will have to be done across a broader range of treatments to elucidate the effects of ethosomal triterpenes on tyrosinase activity. The established therapeutic potential of these triterpenes towards a variety of afflictions affecting the skin combined with the proven capabilities of ethosomes as transdermal drug carriers support their use in the future development of topical applications.

Conclusion

Betulin and betulinic acid are pentacyclic triterpenes with selective cytotoxicity towards melanoma and established anti-melanogenic effects. Their poor hydrosolubility has hindered their attractiveness for use in pharmaceutical and cosmetic formulations. The results of this study demonstrate that these triterpenes can be incorporated into ethosomes with high efficiency to improve the potential delivery and bioavailability of these compounds. Furthermore, ethosomal formulations of BE and BA were shown to exhibit enhanced anti-melanoma effect in B16 melanoma cells when compared to their free forms in solution. A triterpene extract from *Betula papyrifera* was also investigated and shown to have similar cytotoxicity towards B16 melanoma cells as the pure triterpenes. The anti-melanogenic effects of betulin, betulinic acid, and the triterpene extract were assessed based on their ability to inhibit cellular tyrosinase in B16-F10 melanoma cells and were all shown to inhibit the activity of the enzyme more effectively than the standard control kojic acid, though no improvement in anti-melanogenic effect was observed when the compounds were delivered in ethosomes. These preliminary results suggest that further studies examining the use of ethosomal carriers for the delivery of these triterpenes are warranted, and the potential of these compounds as anti-melanoma and anti-melanogenic agents should be further explored, especially in topical applications.

References

[1] X. Yu, L. Du, Y. Li, G. Fu, and Y. Jin, "Improved anti-melanoma effect of a transdermal mitoxantrone ethosome gel," *Biomed. Pharmacother.*, vol. 73, no. Supplement C, pp. 6–11, Jul. 2015.

[2] H. Gogas, A. Polyzos, and J. Kirkwood, "Immunotherapy for advanced melanoma: fulfilling the promise," *Cancer Treat. Rev.*, vol. 39, no. 8, pp. 879–885, Dec. 2013.

[3] E. Pisha *et al.*, "Discovery of betulinic acid as a selective inhibitor of human melanoma that functions by induction of apoptosis," *Nat. Med.*, vol. 1, no. 10, pp. 1046–1051, Oct. 1995.

[4] W.-K. Liu, J. C. K. Ho, F. W. K. Cheung, B. P. L. Liu, W.-C. Ye, and C.-T. Che, "Apoptotic activity of betulinic acid derivatives on murine melanoma B16 cell line," *Eur. J. Pharmacol.*, vol. 498, no. 1, pp. 71–78, Sep. 2004.

[5] D. S. H. L. Kim, J. M. Pezzuto, and E. Pisha, "Synthesis of betulinic acid derivatives with activity against human melanoma," *Bioorg. Med. Chem. Lett.*, vol. 8, no. 13, pp. 1707–1712, Jul. 1998.

[6] S. S. Bodade, K. S. Shaikh, M. S. Kamble, and P. D. Chaudhari, "A study on ethosomes as mode for transdermal delivery of an antidiabetic drug," *Drug Deliv.*, vol. 20, no. 1, pp. 40–46, Jan. 2013.

[7] X. Zhu, F. Li, X. Peng, and K. Zeng, "Formulation and evaluation of lidocaine base ethosomes for transdermal delivery," *Anesth. Analg.*, vol. 117, no. 2, pp. 352–357, Aug. 2013.

[8] T. Limsuwan, P. Boonme, P. Khongkow, and T. Amnuaikit, "Ethosomes of Phenylethyl Resorcinol as Vesicular Delivery System for Skin Lightening Applications," *BioMed Research International*, 2017. [Online]. Available: https://www.hindawi.com/journals/bmri/2017/8310979/. [Accessed: 14-Nov-2017].

[9] Canadian Cancer Society's Advisory and Committee on Cancer Statistics, "Canadian Cancer Statistics 2014," *Can. Cancer Soc.*, 2014.

[10] Canadian Cancer Society's Advisory Committee on Cancer Statistics, "Canadian Cancer Statistics 2017," : *cancer.ca/Canadian-CancerStatistics-2017-EN.pdf*, Jun-2017. .

[11] M. Situm, M. Buljan, S. O. Bulić, and D. Simić, "The mechanisms of UV radiation in the development of malignant melanoma," *Coll. Antropol.*, vol. 31 Suppl 1, pp. 13–16, Jan. 2007.

[12] R. R. Mehta *et al.*, "In vitro transformation of human congenital naevus to malignant melanoma," *Melanoma Res.*, vol. 12, no. 1, pp. 27–33, 2002.

[13] J. W. Little, "Melanoma: etiology, treatment, and dental implications," *Gen. Dent.*, vol. 54, no. 1, pp. 61–66; quiz, 67, Feb. 2006.

[14] K. Volkovova, D. Bilanicova, A. Bartonova, S. Letašiová, and M. Dusinska, "Associations between environmental factors and incidence of cutaneous melanoma. Review," *Environ. Health*, vol. 11, no. 1, p. S12, 2012.

[15] V. J. Cogliano *et al.*, "Preventable Exposures Associated With Human Cancers," *JNCI J. Natl. Cancer Inst.*, vol. 103, no. 24, pp. 1827–1839, Dec. 2011.

[16] L. K. Dennis, M. J. VanBeek, L. E. Beane Freeman, B. J. Smith, D. V. Dawson, and J. A. Coughlin, "Sunburns and risk of cutaneous melanoma, does age matter: a comprehensive meta-analysis," *Ann. Epidemiol.*, vol. 18, no. 8, pp. 614–627, Aug. 2008.

[17] R. Zanetti *et al.*, "Comparison of risk patterns in carcinoma and melanoma of the skin in men: a multi-centre case–case–control study," *Br. J. Cancer*, vol. 94, no. 5, pp. 743–751, Mar. 2006.

[18] F. E. Ghissassi *et al.*, "A review of human carcinogens—Part D: radiation," *Lancet Oncol.*, vol. 10, no. 8, pp. 751–752, Aug. 2009.

[19] J. A. Levine, M. Sorace, J. Spencer, and D. M. Siegel, "The indoor UV tanning industry: a review of skin cancer risk, health benefit claims, and regulation," *J. Am. Acad. Dermatol.*, vol. 53, no. 6, pp. 1038–1044, Dec. 2005.

[20] M. R. Wehner, M. L. Shive, M.-M. Chren, J. Han, A. A. Qureshi, and E. Linos, "Indoor tanning and non-melanoma skin cancer: systematic review and meta-analysis," *BMJ*, vol. 345, no. oct02 3, pp. e5909–e5909, Oct. 2012.

[21] M. Boniol, P. Autier, P. Boyle, and S. Gandini, "Cutaneous melanoma attributable to sunbed use: systematic review and meta-analysis," *BMJ*, vol. 345, no. jul24 2, pp. e4757–e4757, Jul. 2012.

[22] D. Scherer and R. Kumar, "Genetics of pigmentation in skin cancer — A review," *Mutat. Res. Mutat. Res.*, vol. 705, no. 2, pp. 141–153, Oct. 2010.

[23] R. P. Gallagher *et al.*, "Sunlight exposure, pigmentary factors, and risk of nonmelanocytic skin cancer. I. Basal cell carcinoma," *Arch. Dermatol.*, vol. 131, no. 2, pp. 157–163, Feb. 1995.

[24] R. Younes, F. C. Abrao, and J. Gross, "Pulmonary metastasectomy for malignant melanoma: prognostic factors for long-term survival," *Melanoma Res.*, vol. 23, no. 4, pp. 307–311, Aug. 2013.

[25] C. Verhoef, J. H. W. de Wilt, D. J. Grünhagen, A. N. van Geel, T. L. M. ten Hagen, and A. M. M. Eggermont, "Isolated Limb Perfusion with Melphalan and TNF-α in the Treatment of Extremity Sarcoma," *Curr. Treat. Options Oncol.*, vol. 8, no. 6, pp. 417–427, Dec. 2007.

[26] H. E. John and P. J. Mahaffey, "Laser ablation and cryotherapy of melanoma metastases," *J. Surg. Oncol.*, vol. 109, no. 4, pp. 296–300, Mar. 2014.

[27] G. Delaney, M. Barton, and S. Jacob, "Estimation of an optimal radiotherapy utilization rate for melanoma: a review of the evidence," *Cancer*, vol. 100, no. 6, pp. 1293–1301, Mar. 2004.

[28] A. Ribas and K. T. Flaherty, “BRAF targeted therapy changes the treatment paradigm in melanoma,” *Nat. Rev. Clin. Oncol.*, vol. 8, no. 7, pp. 426–433, 2011.

[29] B. Krone, K. F. Kölmel, B. M. Henz, and J. M. Grange, “Protection against melanoma by vaccination with Bacille Calmette-Guerin (BCG) and/or vaccinia: an epidemiology-based hypothesis on the nature of a melanoma risk factor and its immunological control,” *Eur. J. Cancer Oxf. Engl. 1990*, vol. 41, no. 1, pp. 104–117, Jan. 2005.

[30] D. Pirard, M. Heenen, C. Melot, and P. Vereecken, “Interferon Alpha as Adjuvant Postsurgical Treatment of Melanoma: A Meta-Analysis,” *Dermatology*, vol. 208, no. 1, pp. 43–48, 2004.

[31] T. L. Whiteside, P. Schuler, and B. Schilling, “Induced and natural regulatory T cells in human cancer,” *Expert Opin. Biol. Ther.*, vol. 12, no. 10, pp. 1383–1397, Oct. 2012.

[32] S. A. Rosenberg *et al.*, “Durable complete responses in heavily pretreated patients with metastatic melanoma using T-cell transfer immunotherapy,” *Clin. Cancer Res. Off. J. Am. Assoc. Cancer Res.*, vol. 17, no. 13, pp. 4550–4557, Jul. 2011.

[33] M. E. Sehl and F. E. Yates, “Kinetics of Human AgingI. Rates of Senescence Between Ages 30 and 70 Years in Healthy People,” *J. Gerontol. Ser. A*, vol. 56, no. 5, pp. B198–B208, May 2001.

[34] M. Royer, M. Prado, M. E. García-Pérez, P. N. Diouf, and T. Stevanovic, “Study of nutraceutical, nutricosmetics and cosmeceutical potentials of polyphenolic bark extracts from Canadian forest species,” *PharmaNutrition*, vol. 1, no. 4, pp. 158–167, Oct. 2013.

[35] H. S. Datta, S. K. Mitra, R. Paramesh, and B. Patwardhan, “Theories and Management of Aging: Modern and Ayurveda Perspectives,” *Evid.-Based Complement. Altern. Med. ECAM*, vol. 2011, 2011.

[36] G. Péterszegi, N. Isnard, A. M. Robert, and L. Robert, “Studies on skin aging. Preparation and properties of fucose-rich oligo- and polysaccharides. Effect on fibroblast proliferation and survival,” *Biomed. Pharmacother.*, vol. 57, no. 5, pp. 187–194, Jul. 2003.

[37] J. Bhawan, W. Andersen, J. Lee, R. Labadie, and G. Solares, “Photoaging versus intrinsic aging: A morphologic assessment of facial skin*,” *J. Cutan. Pathol.*, vol. 22, no. 2, pp. 154–159, Apr. 1995.

[38] N. Sultana and N. H. Lee, “Antielastase and free radical scavenging activities of compounds from the stems of Cornus kousa,” *Phytother. Res.*, vol. 21, no. 12, pp. 1171–1176, Dec. 2007.

[39] J. j. Leyden, B. Shergill, G. Micali, J. Downie, and W. Wallo, “Natural options for the management of hyperpigmentation,” *J. Eur. Acad. Dermatol. Venereol.*, vol. 25, no. 10, pp. 1140–1145, Oct. 2011.

[40] C. Olivares, C. Jiménez-Cervantes, J. A. Lozano, F. Solano, and J. C. García-Borrón, “The 5,6-dihydroxyindole-2-carboxylic acid (DHICA) oxidase activity of human tyrosinase.,” *Biochem. J.*, vol. 354, no. Pt 1, pp. 131–139, Feb. 2001.

[41] A. Palumbo, M. d'Ischia, G. Misuraca, and G. Prota, "Mechanism of inhibition of melanogenesis by hydroquinone," *Biochim. Biophys. Acta*, vol. 1073, no. 1, pp. 85–90, Jan. 1991.

[42] K. Maeda and M. Fukuda, "Arbutin: mechanism of its depigmenting action in human melanocyte culture," *J. Pharmacol. Exp. Ther.*, vol. 276, no. 2, pp. 765–769, Feb. 1996.

[43] J. Cabanes, S. Chazarra, and F. Garcia-Carmona, "Kojic acid, a cosmetic skin whitening agent, is a slow-binding inhibitor of catecholase activity of tyrosinase," *J. Pharm. Pharmacol.*, vol. 46, no. 12, pp. 982–985, Dec. 1994.

[44] M. I. Rendon and J. I. Gaviria, "Review of skin-lightening agents," *Dermatol. Surg. Off. Publ. Am. Soc. Dermatol. Surg. Al*, vol. 31, no. 7 Pt 2, pp. 886–889; discussion 889, Jul. 2005.

[45] S. Rastogi, M. M. Pandey, and A. Kumar Singh Rawat, "Medicinal plants of the genus Betula—Traditional uses and a phytochemical–pharmacological review," *J. Ethnopharmacol.*, vol. 159, pp. 62–83, Jan. 2015.

[46] S. Ciurlea, C. Soica, D. Ionescu, R. Ambrus, S. Feflea, and C. A. Dehelean, "Birch tree outer bark, a natural source of bioactive pentacyclic triterpenes with an antitumor activity," *J Agroalim Proc Technol*, vol. 16, pp. 328–332, 2010.

[47] P. Yogeeswari and D. Sriram, "Betulinic acid and its derivatives: a review on their biological properties," *Curr. Med. Chem.*, vol. 12, no. 6, pp. 657–666, 2005.

[48] P. A. Krasutsky, "Birch bark research and development," *Nat. Prod. Rep.*, vol. 23, no. 6, p. 919, 2006.

[49] F. Bouvier, A. Rahier, and B. Camara, "Biogenesis, molecular regulation and function of plant isoprenoids," *Prog. Lipid Res.*, vol. 44, no. 6, pp. 357–429, Nov. 2005.

[50] Y. Zhang, X. Wu, Y. Ren, J. Fu, and Y. Zhang, "Safety evaluation of a triterpenoid-rich extract from bamboo shavings," *Food Chem. Toxicol. Int. J. Publ. Br. Ind. Biol. Res. Assoc.*, vol. 42, no. 11, pp. 1867–1875, Nov. 2004.

[51] J. Patočka, "Biologically active pentacyclic triterpenes and their current medicine signification," *J Appl Biomed*, vol. 1, no. 1, pp. 7–12, 2003.

[52] M. Hassegawa, T. Stevanovic, and A. Achim, "Relationship between ethanolic extracts of yellow birch and tree characteristics," *Ind. Crops Prod.*, vol. 94, pp. 1–8, Dec. 2016.

[53] J. Yin *et al.*, "Effect of MeJA and light on the accumulation of betulin and oleanolic acid in the saplings of white birch (Betula platyphylla Suk.)," *Am. J. Plant Sci.*, vol. 4, no. 12, p. 7, 2013.

[54] M. Recio, R. Giner, S. Máñez, and J. L Ríos, "Structural Requirements for the Anti-Inflammatory Activity of Natural Triterpenoids," *Planta Med.*, vol. 61, pp. 182–5, May 1995.

[55] N. Miura, Y. Matsumoto, S. Miyairi, S. Nishiyama, and A. Naganuma, “Protective effects of triterpene compounds against the cytotoxicity of cadmium in HepG2 cells,” *Mol. Pharmacol.*, vol. 56, no. 6, pp. 1324–1328, Dec. 1999.

[56] S. K. Król, M. Kiełbus, A. Rivero-Müller, and A. Stepulak, “Comprehensive Review on Betulin as a Potent Anticancer Agent,” *BioMed Research International*, 2015. [Online]. Available: https://www.hindawi.com/journals/bmri/2015/584189/. [Accessed: 10-Feb-2018].

[57] C. Şoica, “Betulin – A Future Key-Player in the Treatment of Neoplasic Diseases,” *Med. Aromat. Plants*, vol. 01, no. 08, 2012.

[58] C. Gauthier, J. Legault, S. Lavoie, S. Rondeau, S. Tremblay, and A. Pichette, “Synthesis and Cytotoxicity of Bidesmosidic Betulin and Betulinic Acid Saponins,” *J. Nat. Prod.*, vol. 72, no. 1, pp. 72–81, Jan. 2009.

[59] W. Rzeski *et al.*, “Betulin Elicits Anti-Cancer Effects in Tumour Primary Cultures and Cell Lines In Vitro,” *Basic Clin. Pharmacol. Toxicol.*, vol. 105, no. 6, pp. 425–432, Dec. 2009.

[60] J. Sung Pyo *et al.*, “Anti-Cancer Effect of Betulin on a Human Lung Cancer Cell Line: A Pharmacoproteomic Approach Using 2 D SDS PAGE Coupled with Nano-HPLC Tandem Mass Spectrometry,” *Planta Med.*, vol. 75, pp. 127–31, Feb. 2009.

[61] Y. Li *et al.*, “Betulin induces mitochondrial cytochrome c release associated apoptosis in human cancer cells,” *Mol. Carcinog.*, vol. 49, no. 7, pp. 630–640, Jul. 2010.

[62] K. Hata, K. Hori, H. Ogasawara, and S. Takahashi, “Anti-leukemia activities of Lup-28-al-20(29)-en-3-one, a lupane triterpene,” *Toxicol. Lett.*, vol. 143, no. 1, pp. 1–7, Jun. 2003.

[63] C. Gauthier, J. Legault, M. Lebrun, P. Dufour, and A. Pichette, “Glycosidation of lupane-type triterpenoids as potent in vitro cytotoxic agents,” *Bioorg. Med. Chem.*, vol. 14, no. 19, pp. 6713–6725, Oct. 2006.

[64] K. Hata, K. Hori, and S. Takahashi, “Differentiation- and Apoptosis-Inducing Activities by Pentacyclic Triterpenes on a Mouse Melanoma Cell Line,” *J. Nat. Prod.*, vol. 65, no. 5, pp. 645–648, May 2002.

[65] C. Şoica *et al.*, “Betulin Complex in γ-Cyclodextrin Derivatives: Properties and Antineoplasic Activities in In Vitro and In Vivo Tumor Models,” *Int. J. Mol. Sci.*, vol. 13, no. 11, pp. 14992–15011, Nov. 2012.

[66] J. Sarek, M. Kvasnica, M. Urban, J. Klinot, and M. Hajduch, “Correlation of cytotoxic activity of betulinines and their hydroxy analogues,” *Bioorg. Med. Chem. Lett.*, vol. 15, no. 19, pp. 4196–4200, Oct. 2005.

[67] C. A. Dehelean, S. Feflea, J. Molnár, I. Zupko, and C. Soica, “Betulin as an antitumor agent tested in vitro on A431, HeLa and MCF7, and as an angiogenic inhibitor in vivo in the CAM assay,” *Nat. Prod. Commun.*, vol. 7, no. 8, pp. 981–985, Aug. 2012.

[68] C. Mutai, “Cytotoxic lupane-type triterpenoids from Acacia mellifera,” *Phytochemistry*, vol. 65, no. 8, pp. 1159–1164, Apr. 2004.

[69] S. Elmore, “Apoptosis: A Review of Programmed Cell Death,” *Toxicol. Pathol.*, vol. 35, no. 4, pp. 495–516, Jun. 2007.

[70] F. B. Mullauer, J. H. Kessler, and J. P. Medema, “Betulin Is a Potent Anti-Tumor Agent that Is Enhanced by Cholesterol,” *PLOS ONE*, vol. 4, no. 4, p. e1, Apr. 2009.

[71] S. A. Kuznetsova, G. P. Skvortsova, I. N. Maliar, E. S. Skurydina, and O. F. Veselova, “Extraction of betulin from birch bark and study of its physico-chemical and pharmacological properties,” *Russ. J. Bioorganic Chem.*, vol. 40, no. 7, pp. 742–747, Dec. 2014.

[72] C. Huyke, M. Laszczyk, A. Scheffler, R. Ernst, and C. M. Schempp, “Treatment of actinic keratoses with birch bark extract: a pilot study,” *JDDG J. Dtsch. Dermatol. Ges.*, vol. 4, no. 2, pp. 132–136, Feb. 2006.

[73] C. Huyke *et al.*, “Treatment of actinic keratoses with a novel betulin-based oleogel. A prospective, randomized, comparative pilot study,” *JDDG J. Dtsch. Dermatol. Ges.*, vol. 7, no. 2, pp. 128–133, Feb. 2009.

[74] W. Fu and C. J. Cockerell, “The Actinic (Solar) Keratosis: A 21st-Century Perspective,” *Arch. Dermatol.*, vol. 139, no. 1, pp. 66–70, Jan. 2003.

[75] F. Retzlaff, “Ueber Herba Gratiolae,” *Arch. Pharm. (Weinheim)*, vol. 240, no. 8, pp. 561–568, Jan. 1902.

[76] A. Robertson, G. Soliman, and E. C. Owen, “269. Polyterpenoid compounds. Part I. Betulic acid from Cornus florida, L.,” *J. Chem. Soc. Resumed*, pp. 1267–1273, 1939.

[77] M. C. Recio *et al.*, “Investigations on the steroidal anti-inflammatory activity of triterpenoids from Diospyros leucomelas,” *Planta Med.*, vol. 61, no. 1, pp. 9–12, Feb. 1995.

[78] C.-W. Chang, T.-S. Wu, Y.-S. Hsieh, S.-C. Kuo, and P.-D. L. Chao, “Terpenoids of Syzygium formosanum,” *J. Nat. Prod.*, vol. 62, no. 2, pp. 327–328, Feb. 1999.

[79] B. Nyasse, J.-J. Nono, Y. Nganso, I. Ngantchou, and B. Schneider, “Uapaca genus (Euphorbiaceae), a good source of betulinic acid,” *Fitoterapia*, vol. 80, no. 1, pp. 32–34, Jan. 2009.

[80] A. Ikuta, K. Kamiya, T. Satake, and Y. Saiki, “Triterpenoids from callus tissue cultures of Paeonia species,” *Phytochemistry*, vol. 38, no. 5, pp. 1203–1207, Mar. 1995.

[81] A. Barthel, S. Stark, and R. Csuk, “Oxidative transformations of betulinol,” *Tetrahedron*, vol. 39, no. 64, pp. 9225–9229, 2008.

[82] R. Csuk, “Betulinic acid and its derivatives: a patent review (2008-2013),” *Expert Opin. Ther. Pat.*, vol. 24, no. 8, pp. 913–923, Aug. 2014.

[83] M. L. Schmidt, K. L. Kuzmanoff, L. Ling-Indeck, and J. M. Pezzuto, “Betulinic acid induces apoptosis in human neuroblastoma cell lines,” *Eur. J. Cancer Oxf. Engl. 1990*, vol. 33, no. 12, pp. 2007–2010, Oct. 1997.

[84] S. Fulda, I. Jeremias, T. Pietsch, and K. M. Debatin, “Betulinic acid: a new chemotherapeutic agent in the treatment of neuroectodermal tumors,” *Klin. Padiatr.*, vol. 211, no. 4, pp. 319–322, Aug. 1999.

[85] W. Wick, C. Grimmel, B. Wagenknecht, J. Dichgans, and M. Weller, “Betulinic acid-induced apoptosis in glioma cells: A sequential requirement for new protein synthesis, formation of reactive oxygen species, and caspase processing,” *J. Pharmacol. Exp. Ther.*, vol. 289, no. 3, pp. 1306–1312, Jun. 1999.

[86] D. Thurnher *et al.*, “Betulinic acid: A new cytotoxic compound against malignant head and neck cancer cells,” *Head Neck*, vol. 25, no. 9, pp. 732–740, Sep. 2003.

[87] J. Y. Kim, H. M. Koo, and D. S. Kim, “Development of C-20 modified betulinic acid derivatives as antitumor agents,” *Bioorg. Med. Chem. Lett.*, vol. 11, no. 17, pp. 2405–2408, Sep. 2001.

[88] E. Selzer *et al.*, “Effects of Betulinic Acid Alone and in Combination with Irradiation in Human Melanoma Cells,” *J. Invest. Dermatol.*, vol. 114, no. 5, pp. 935–940, May 2000.

[89] Y. Gao *et al.*, “Combining betulinic acid and mithramycin a effectively suppresses pancreatic cancer by inhibiting proliferation, invasion, and angiogenesis,” *Cancer Res.*, vol. 71, no. 15, pp. 5182–5193, Aug. 2011.

[90] N. Sawada *et al.*, “Betulinic acid augments the inhibitory effects of vincristine on growth and lung metastasis of B16F10 melanoma cells in mice,” *Br. J. Cancer*, vol. 90, no. 8, pp. 1672–1678, Apr. 2004.

[91] P. Wang *et al.*, “Betulinic acid exerts immunoregulation and anti-tumor effect on cervical carcinoma (U14) tumor-bearing mice,” *Pharm.*, vol. 67, no. 8, pp. 733–739, Aug. 2012.

[92] L. Potze, F. B. Mullauer, S. Colak, J. H. Kessler, and J. P. Medema, “Betulinic acid-induced mitochondria-dependent cell death is counterbalanced by an autophagic salvage response,” *Cell Death Dis.*, vol. 5, p. e1169, Apr. 2014.

[93] R. H. Cichewicz and S. A. Kouzi, “Chemistry, biological activity, and chemotherapeutic potential of betulinic acid for the prevention and treatment of cancer and HIV infection,” *Med. Res. Rev.*, vol. 24, no. 1, pp. 90–114, Jan. 2004.

[94] F. Sandberg, H. Dutschewska, V. Christov, and S. Spassov, "Spondianthus preussii var. glaber Engler. Pharmacological screening and occurrence of triterpenes," *Acta Pharm. Suec.*, vol. 24, no. 5, pp. 253–256, 1987.

[95] T. Galgon, W. Wohlrab, and B. Dräger, "Betulinic acid induces apoptosis in skin cancer cells and differentiation in normal human keratinocytes," *Exp. Dermatol.*, vol. 14, no. 10, pp. 736–743, Oct. 2005.

[96] W. Rzeski *et al.*, "Betulinic acid decreases expression of bcl-2 and cyclin D1, inhibits proliferation, migration and induces apoptosis in cancer cells," *Naunyn. Schmiedebergs Arch. Pharmacol.*, vol. 374, no. 1, pp. 11–20, Oct. 2006.

[97] J. H. Kim, J. C. Byun, C.-G. Hyun, and N. H. Lee, "Compounds with elastase inhibition and free radical scavenging activities from Callistemon lanceolatus," *J. Med. Plants Res.*, vol. 3, no. 11, pp. 914–920, 2009.

[98] S. Iravani and B. Zolfaghari, "Pharmaceutical and nutraceutical effects of Pinus pinaster bark extract," *Res. Pharm. Sci.*, vol. 6, no. 1, pp. 1–11, Jan. 2011.

[99] F. Ullah *et al.*, "Tyrosinase inhibitory pentacyclic triterpenes and analgesic and spasmolytic activities of methanol extracts of Rhododendron collettianum," *Phytother. Res. PTR*, vol. 21, no. 11, pp. 1076–1081, Nov. 2007.

[100] I. M. Abdulbaqi, Y. Darwis, N. A. K. Khan, R. A. Assi, and A. A. Khan, "Ethosomal nanocarriers: the impact of constituents and formulation techniques on ethosomal properties, in vivo studies, and clinical trials," *Int. J. Nanomedicine*, vol. 11, pp. 2279–2304, May 2016.

[101] M. R. Prausnitz and R. Langer, "Transdermal drug delivery," *Nat. Biotechnol.*, vol. 26, no. 11, pp. 1261–1268, Nov. 2008.

[102] C. M. Schoellhammer, D. Blankschtein, and R. Langer, "Skin Permeabilization for Transdermal Drug Delivery: Recent Advances and Future Prospects," *Expert Opin. Drug Deliv.*, vol. 11, no. 3, pp. 393–407, Mar. 2014.

[103] L. Sercombe, T. Veerati, F. Moheimani, S. Y. Wu, A. K. Sood, and S. Hua, "Advances and Challenges of Liposome Assisted Drug Delivery," *Front. Pharmacol.*, vol. 6, Dec. 2015.

[104] G. A. Koning and G. Storm, "Targeted drug delivery systems for the intracellular delivery of macromolecular drugs," *Drug Discov. Today*, vol. 8, no. 11, pp. 482–483, Jun. 2003.

[105] S. Hua and P. J. Cabot, "Targeted nanoparticles that mimic immune cells in pain control inducing analgesic and anti-inflammatory actions: a potential novel treatment of acute and chronic pain condition," *Pain Physician*, vol. 16, no. 3, pp. E199-216, Jun. 2013.

[106] Y. Hashimoto and S. Suzuki, "Basic approach to application of liposomes for cancer chemotherapy," *Tohoku J. Exp. Med.*, vol. 168, no. 2, pp. 361–369, 1992.

[107] J. M. López-Pinto, M. L. González-Rodríguez, and A. M. Rabasco, "Effect of cholesterol and ethanol on dermal delivery from DPPC liposomes," *Int. J. Pharm.*, vol. 298, no. 1, pp. 1–12, Jul. 2005.

[108] E. Touitou, N. Dayan, L. Bergelson, B. Godin, and M. Eliaz, "Ethosomes — novel vesicular carriers for enhanced delivery: characterization and skin penetration properties," *J. Controlled Release*, vol. 65, no. 3, pp. 403–418, Apr. 2000.

[109] E. Touitou, M. Alkabes, N. Dayan, and M. Eliaz, "Ethosomes: novel vesicular carriers for enhanced skin delivery," *Pharm Res*, vol. 14, pp. S305–S306, 1997.

[110] E. R. Bendas and M. I. Tadros, "Enhanced transdermal delivery of salbutamol sulfate via ethosomes," *AAPS PharmSciTech*, vol. 8, no. 4, Oct. 2007.

[111] B. C. Finnin and T. M. Morgan, "Transdermal penetration enhancers: applications, limitations, and potential," *J. Pharm. Sci.*, vol. 88, no. 10, pp. 955–958, Oct. 1999.

[112] B. Godin and E. Touitou, "Mechanism of bacitracin permeation enhancement through the skin and cellular membranes from an ethosomal carrier," *J. Controlled Release*, vol. 94, no. 2, pp. 365–379, Feb. 2004.

[113] E. Touitou, B. Godin, N. Dayan, C. Weiss, A. Piliponsky, and F. Levi-Schaffer, "Intracellular delivery mediated by an ethosomal carrier," *Biomaterials*, vol. 22, no. 22, pp. 3053–3059, Nov. 2001.

[114] R. Puri and S. Jain, "Ethogel topical formulation for increasing the local bioavailability of 5-fluorouracil: a mechanistic study," *Anticancer Drugs*, vol. 23, no. 9, pp. 923–934, Oct. 2012.

[115] R. Rakesh and K. R. Anoop, "Formulation and optimization of nano-sized ethosomes for enhanced transdermal delivery of cromolyn sodium," *J. Pharm. Bioallied Sci.*, vol. 4, no. 4, pp. 333–340, 2012.

[116] M. Chen, X. Liu, and A. Fahr, "Skin penetration and deposition of carboxyfluorescein and temoporfin from different lipid vesicular systems: In vitro study with finite and infinite dosage application," *Int. J. Pharm.*, vol. 408, no. 1–2, pp. 223–234, Apr. 2011.

[117] T. Limsuwan and T. Amnuaikit, "Development of Ethosomes Containing Mycophenolic Acid," *Procedia Chem.*, vol. 4, pp. 328–335, Jan. 2012.

[118] A. Ahad, M. Aqil, K. Kohli, Y. Sultana, and M. Mujeeb, "Enhanced transdermal delivery of an anti-hypertensive agent via nanoethosomes: statistical optimization, characterization and pharmacokinetic assessment," *Int. J. Pharm.*, vol. 443, no. 1–2, pp. 26–38, Feb. 2013.

[119] Z. Zhang *et al.*, "In vitro study of ethosome penetration in human skin and hypertrophic scar tissue," *Nanomedicine Nanotechnol. Biol. Med.*, vol. 8, no. 6, pp. 1026–1033, Aug. 2012.

[120] S. Shen *et al.*, "Compound antimalarial ethosomal cataplasm: preparation, evaluation, and mechanism of penetration enhancement," *Int. J. Nanomedicine*, vol. 10, pp. 4239–4253, 2015.

[121] C. K. Song, P. Balakrishnan, C.-K. Shim, S.-J. Chung, S. Chong, and D.-D. Kim, "A novel vesicular carrier, transethosome, for enhanced skin delivery of voriconazole: characterization and in vitro/in vivo evaluation," *Colloids Surf. B Biointerfaces*, vol. 92, pp. 299–304, Apr. 2012.

[122] M. Ma, J. Wang, F. Guo, M. Lei, F. Tan, and N. Li, "Development of nanovesicular systems for dermal imiquimod delivery: physicochemical characterization and in vitro/in vivo evaluation," *J. Mater. Sci. Mater. Med.*, vol. 26, no. 6, p. 191, Jun. 2015.

[123] Y.-Z. Zhao *et al.*, "Selection of high efficient transdermal lipid vesicle for curcumin skin delivery," *Int. J. Pharm.*, vol. 454, no. 1, pp. 302–309, Sep. 2013.

[124] Y. Zhang, W. Ng, J. Hu, S. S. Mussa, Y. Ge, and H. Xu, "Formulation and in vitro stability evaluation of ethosomal carbomer hydrogel for transdermal vaccine delivery," *Colloids Surf. B Biointerfaces*, vol. 163, pp. 184–191, Mar. 2018.

[125] S. Mahmood, U. K. Mandal, and B. Chatterjee, "Transdermal delivery of raloxifene HCl via ethosomal system: Formulation, advanced characterizations and pharmacokinetic evaluation," *Int. J. Pharm.*, vol. 542, no. 1, pp. 36–46, May 2018.

[126] B. Nagadevi, K. S. Kumar, P. Venkanna, and D. Prabhakar, "Formulation and characterisation of Tizanidine hydrochloride loaded ethosomes patch," *Int. J. Pharm. Pharm. Sci.*, vol. 6, pp. 199–205, Jan. 2014.

[127] X. Liu *et al.*, "Preparation of a ligustrazine ethosome patch and its evaluation in vitro and in vivo," *Int. J. Nanomedicine*, vol. 6, pp. 241–247, 2011.

[128] H. Mulani and K. Bhise, "QbD Approach in the formulation and evaluation of Miconazole Nitrate loaded ethosomal cream-o-gel," *Int Res J Pharm Sci*, vol. 8, pp. 1–37, 2017.

[129] T. Mosmann, "Rapid colorimetric assay for cellular growth and survival: application to proliferation and cytotoxicity assays," *J. Immunol. Methods*, vol. 65, no. 1–2, pp. 55–63, Dec. 1983.

[130] Y. Tomita, K. Maeda, and H. Tagami, "Melanocyte-Stimulating Properties of Arachidonic Acid Metabolites: Possible Role in Postinflammatory Pigmentation," *Pigment Cell Res.*, vol. 5, no. 5, pp. 357–361, Nov. 1992.

[131] J.-G. Chen, Y.-F. Liu, and T.-W. Gao, "Preparation and anti-inflammatory activity of triptolide ethosomes in an erythema model," *J. Liposome Res.*, vol. 20, no. 4, pp. 297–303, Dec. 2010.

[132] "Particle Size Interpretation: Number vs. Volume Distributions - HORIBA." [Online]. Available: http://www.horiba.com/scientific/products/particle-characterization/education/general-information/data-interpretation/number-vs-volume-distributions/. [Accessed: 01-Mar-2018].

[133] F. B. Mullauer *et al.*, "Betulinic acid delivered in liposomes reduces growth of human lung and colon cancers in mice without causing systemic toxicity:," *Anticancer. Drugs*, vol. 22, no. 3, pp. 223–233, Mar. 2011.

[134] R. Csuk, A. Barthel, R. Kluge, and D. Ströhl, "Synthesis, cytotoxicity and liposome preparation of 28-acetylenic betulin derivatives," *Bioorg. Med. Chem.*, vol. 18, no. 20, pp. 7252–7259, Oct. 2010.

[135] L. B. Son *et al.*, "Synthesis of betulinic acid from betulin and study of its solubilization using liposomes," *Bioorg. Khim.*, vol. 24, no. 10, pp. 787–793, Oct. 1998.

[136] Y. Liu *et al.*, "Antitumor drug effect of betulinic acid mediated by polyethylene glycol modified liposomes," *Mater. Sci. Eng. C*, vol. 64, pp. 124–132, Jul. 2016.

[137] B. Guo, D. Xu, X. Liu, and J. Yi, "Enzymatic synthesis and in vitro evaluation of folate-functionalized liposomes," *Drug Design, Development and Therapy*, 20-Jun-2017. [Online]. Available: https://www.dovepress.com/enzymatic-synthesis-and-in-vitro-evaluation-of-folate-functionalized-l-peer-reviewed-article-DDDT. [Accessed: 23-Mar-2018].

[138] Rodríguez S., Cesio M. V., Heinzen H., and Moyna P., "Determination of the phospholipid/lipophilic compounds ratio in liposomes by thin-layer chromatography scanning densitometry," *Lipids*, vol. 35, no. 9, pp. 1033–1036, Sep. 2000.

[139] J. van Meerloo, G. J. L. Kaspers, and J. Cloos, "Cell Sensitivity Assays: The MTT Assay," in *Cancer Cell Culture*, Humana Press, 2011, pp. 237–245.

[140] Y. Xu and C. Her, "Inhibition of Topoisomerase (DNA) I (TOP1): DNA Damage Repair and Anticancer Therapy," *Biomolecules*, vol. 5, no. 3, pp. 1652–1670, Jul. 2015.

[141] M. Takahashi, D. Kitamoto, Y. Asikin, K. Takara, and K. Wada, "Liposomes encapsulating Aloe vera leaf gel extract significantly enhance proliferation and collagen synthesis in human skin cell lines," *J. Oleo Sci.*, vol. 58, no. 12, pp. 643–650, 2009.

[142] G. Jeswani, "Topical Delivery of Curcuma longa Extract Loaded Nanosized Ethosomes to Combat Facial Wrinkles Research Article," *J. Pharm. Drug Deliv. Res.*, vol. 03, Jan. 2014.

[143] N. Srivastava, K. Srivastava, and A. Singh, "Formulation and evaluation of Seabuckthorn leaf extract loaded ethosomal gels," *Asian J. Pharm. Clin. Res.*, vol. 8, Sep. 2015.

[144] J. Lee *et al.*, "Glycyrrhizin Induces Melanogenesis by Elevating a cAMP Level in B16 Melanoma Cells," *J. Invest. Dermatol.*, vol. 124, no. 2, pp. 405–411, Feb. 2005.

[145] P. T. B. Tu and S. Tawata, "Anti-Oxidant, Anti-Aging, and Anti-Melanogenic Properties of the Essential Oils from Two Varieties of Alpinia zerumbet," *Molecules*, vol. 20, no. 9, pp. 16723–16740, Sep. 2015.

Appendix

Microtrac Flex / Microtrac S3500 Particle Analyzer Data (Vesicle Size)

Table A.1: BE-ethosome particle analysis tabular data from Microtrac Flex software.

	A	B	C
1			
2			
3	**ID1:**	Betulin (3/3)	
4	**ID2:**	-	
5	**Date:**	02/09/2018	
6	**Time:**	16:13	
7	**DB Rec:**	266	
8	**DB Name:**	C:\Program Files\Microtrac FLEX 10.3.15\Databases\MTDatabase.MDB	
9		**Summary Data**	
10		MV(um):	2.450
11		MN(um):	1.449
12		MA(um):	1.501
13		CS:	4.00
14		SD:	0.1150
15			
16		Mz:	1.483
17		si:	0.1201
18		Ski:	0.01142
19		Kg:	1.077
20		**User Defined Calculations**	
21		**Name**	**Value**
22	**Formula 1:**		
23	**Formula 2:**		
24	**Formula 3:**		
25		**Percentiles**	
26		**%Tile**	**Size(um)**
27		10.00	1.327
28		20.00	1.386
29		30.00	1.421
30		40.00	1.452
31		50.00	1.482
32		60.00	1.512
33		70.00	1.545
34		80.00	1.581
35		90.00	1.624
36		95.00	1.691
37		**Size Percent**	
38		**Size(um)**	**%Tile**
39			
40			
41			
42			
43			
44			
45			
46			
47			
48			
49		**Peaks**	
50	**Dia(um)**	**Vol %**	**Width**
51	68.7300	1.20	18.2500
52	3.7700	1.60	17.2100
53	1.4780	97.20	0.2220

Table A.2: BA-ethosome particle analysis tabular data from Microtrac Flex software.

	A	B	C
1			
2			
3	**ID1:**	Betulinic Acid (2/3)	
4	**ID2:**	-	
5	**Date:**	02/08/2018	
6	**Time:**	19:20	
7	**DB Rec:**	235	
8	**DB Name:**	C:\Program Files\Microtrac FLEX 10.3.15\Databases\MTDatabase.MDB	
9	**Summary Data**		
10		MV(um):	4.63
11		MN(um):	1.275
12		MA(um):	2.146
13		CS:	2.795
14		SD:	2.547
15			
16		Mz:	3.45
17		si:	3.46
18		Ski:	0.543
19		Kg:	1.647
20	**User Defined Calculations**		
21		**Name**	**Value**
22	**Formula 1:**		
23	**Formula 2:**		
24	**Formula 3:**		
25	**Percentiles**		
26		**%Tile**	**Size(um)**
27		10.00	1.122
28		20.00	1.236
29		30.00	1.355
30		40.00	1.840
31		50.00	2.875
32		60.00	3.65
33		70.00	4.42
34		80.00	5.50
35		90.00	9.86
36		95.00	15.47
37	**Size Percent**		
38		**Size(um)**	**%Tile**
39			
40			
41			
42			
43			
44			
45			
46			
47			
48			
49	**Peaks**		
50	**Dia(um)**	**Vol %**	**Width**
51	25.3200	5.00	18.8200
52	11.0900	7.40	4.6900
53	3.9700	46.40	2.7770
54	1.2420	41.20	0.4000
55			

Table A.3: TE-ethosomes particle analysis tabular data from Microtrac Flex software.

	A	B	C
1			
2			
3	**ID1:**	Triterpene Extract (2/3)	
4	**ID2:**	-	
5	**Date:**	02/09/2018	
6	**Time:**	16:41	
7	**DB Rec:**	276	
8	**DB Name:**	C:\Program Files\Microtrac FLEX 10.3.15\Databases\MTDatabase.MDB	
9	**Summary Data**		
10		MV(um):	2.947
11		MN(um):	1.783
12		MA(um):	2.419
13		CS:	2.480
14		SD:	1.269
15			
16		Mz:	2.828
17		si:	1.249
18		Ski:	0.2213
19		Kg:	0.902
20	**User Defined Calculations**		
21		**Name**	**Value**
22	**Formula 1:**		
23	**Formula 2:**		
24	**Formula 3:**		
25	**Percentiles**		
26		**%Tile**	**Size(um)**
27		10.00	1.478
28		20.00	1.701
29		30.00	1.969
30		40.00	2.348
31		50.00	2.726
32		60.00	3.08
33		70.00	3.46
34		80.00	3.91
35		90.00	4.63
36		95.00	5.41
37	**Size Percent**		
38		**Size(um)**	**%Tile**
39			
40			
41			
42			
43			
44			
45			
46			
47			
48			
49	**Peaks**		
50	**Dia(um)**	**Vol %**	**Width**
51	3.2500	70.70	2.1360
52	1.5800	29.30	0.4720
53			
54			

Table A.4: Blank Ethosomes particle analysis tabular data from Microtrac Flex software.

	A	B	C
1			
2			
3	**ID1:**	Blank (3/3)	
4	**ID2:**	-	
5	**Date:**	02/08/2018	
6	**Time:**	20:05	
7	**DB Rec:**	251	
8	**DB Name:**	C:\Program Files\Microtrac FLEX 10.3.15\Databases\MTDatabase.MDB	
9	**Summary Data**		
10		MV(um):	3.45
11		MN(um):	1.392
12		MA(um):	1.501
13		CS:	4.00
14		SD:	0.1520
15			
16		Mz:	1.442
17		si:	2.926
18		Ski:	0.473
19		Kg:	37.25
20	**User Defined Calculations**		
21		**Name**	**Value**
22	**Formula 1:**		
23	**Formula 2:**		
24	**Formula 3:**		
25	**Percentiles**		
26		**%Tile**	**Size(um)**
27		10.00	1.250
28		20.00	1.313
29		30.00	1.364
30		40.00	1.406
31		50.00	1.445
32		60.00	1.483
33		70.00	1.524
34		80.00	1.569
35		90.00	1.629
36		95.00	20.02
37	**Size Percent**		
38		**Size(um)**	**%Tile**
39			
40			
41			
42			
43			
44			
45			
46			
47			
48			
49	**Peaks**		
50	**Dia(um)**	**Vol %**	**Width**
51	35.7900	6.00	29.4300
52	1.4340	94.00	0.2800
53			

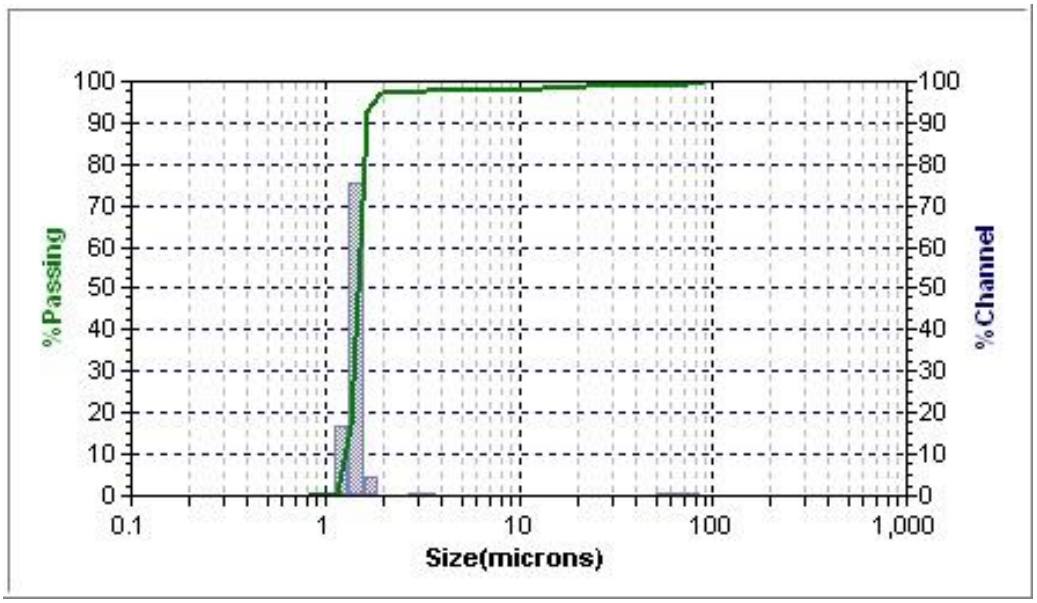

Figure A.1: Particle size distribution of BE-ethosomes produced by Microtrac Flex software

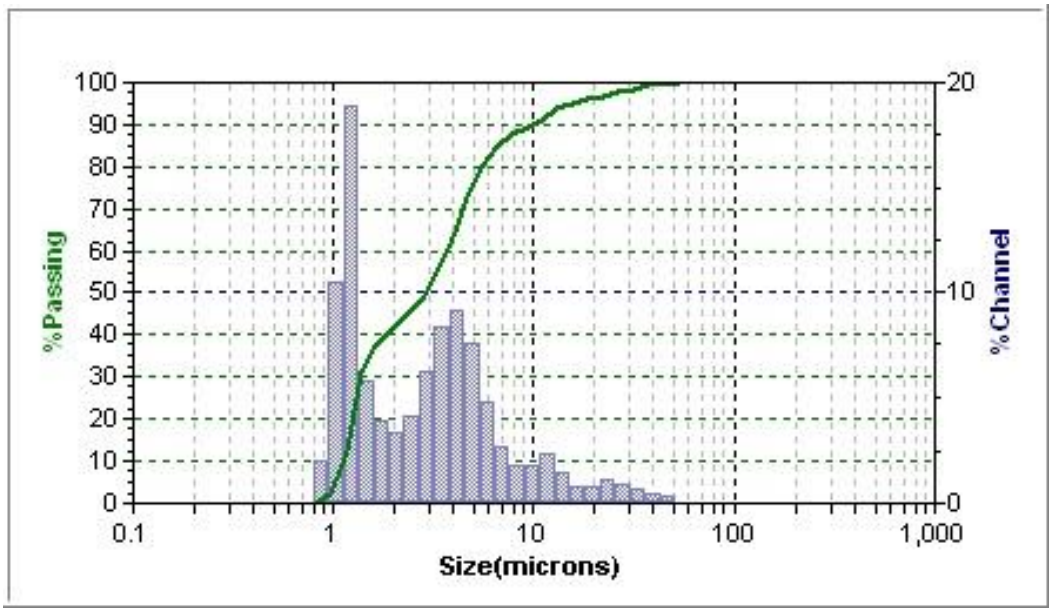

Figure A.2: Particle Size Distribution for BA-ethosomes produced by Microtrac Flex software

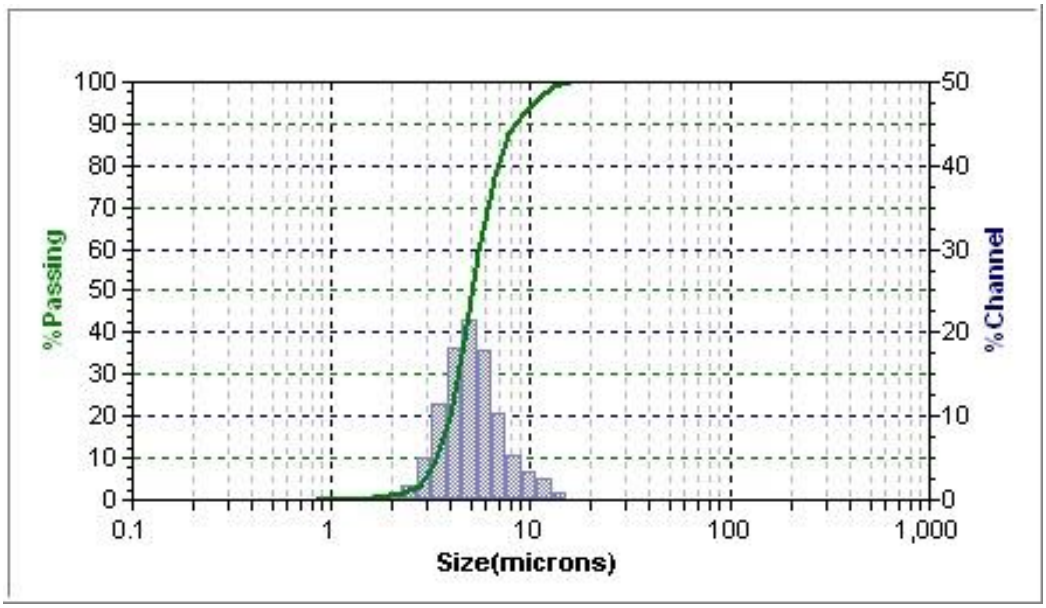

Figure A.3: Particle size distribution of TE-ethosomes produced by Microtrac Flex software.

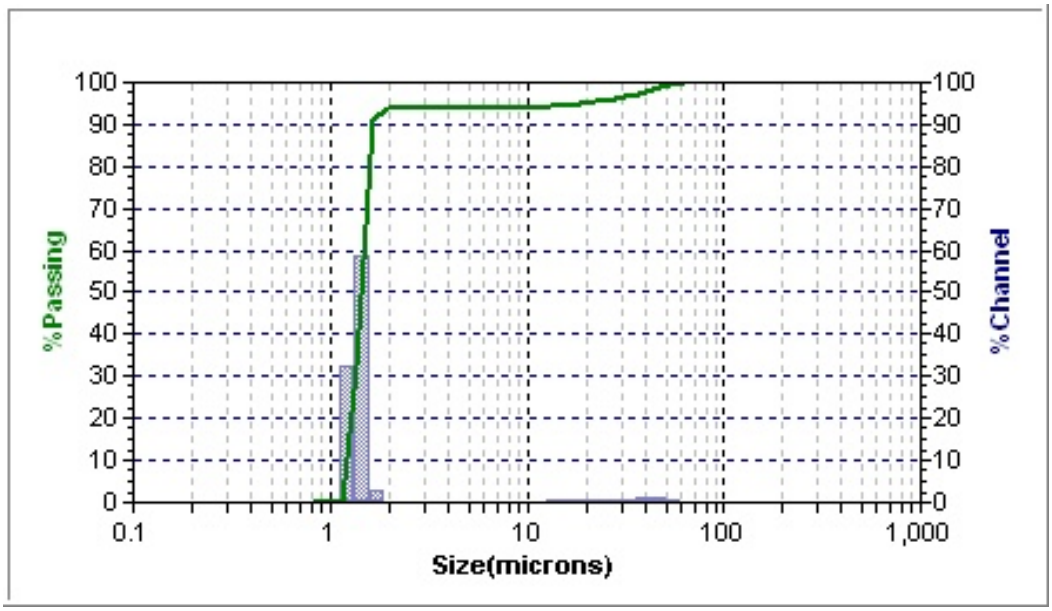

Figure A.4: Particle size distribution for Blank Ethosomes produced by Microtrac Flex software.

Table A.5: Mean vesicle size data from ethosome formulations produced in optimization study as determined using diffraction particle analysis (Microtrac Flex software).

Formulation	MV(um)	SD (um)	Avg (um)	SD (um)
A1	10.36	6.45		
A2	6.51	2.511		
A3	13.77	7.61	10.21333	3.632222
B1	10.15	6.15		
B2	7.46	5.34		
B3	7.88	4.74	8.496667	1.447147
C1	7.76	3.66		
C2	10.23	7.93		
C3	6.83	5.09	8.273333	1.757166
D1	6.76	3.36		
D2	9.16	6.24		
D3	4.09	1.482	6.67	2.536198
E1	3.58	0.937		
E2	3.67	1.311		
E3	3.78	2.35	3.676667	0.100167
F1	4.76	1.802		
F2	4.65	1.934		
F3	3.25	1.33	4.22	0.841843
G1	16.98	11.32		
G2	12.87	6.85		
G3	15.39	8.78	15.08	2.072462
H1	11.32	5.72		
H2	12.21	4.7		
H3	9.46	9.27	10.99667	1.403222
I1	7.95	1.326		
I2	6.7	1.268		
I3	5.36	1.244	6.67	1.295261

Table A.6: Vesicle size data from ethosomes containing triterpenes determined using diffraction particle analysis (Microtrac Flex software).

Formulation	MV(um)	SD (um)	Avg (um)	SD (um)
Betulin	3.71	2.209		
	3.87	1.261		
	2.45	0.115	3.343333	0.777775
Betulinic Acid	5.03	2.978		
	4.63	2.547		
	5.66	3.51	5.106667	0.519262
Triterpene Extract	2.388	0.917		
	2.947	1.269		
	2.372	0.913	2.569	0.327455
Blank	3.68	0.145		
	4.25	0.134		
	3.45	0.152	3.793333	0.411866

HPLC Data (Entrapment Efficiency)

Standard curves for BE, BA, and TE:

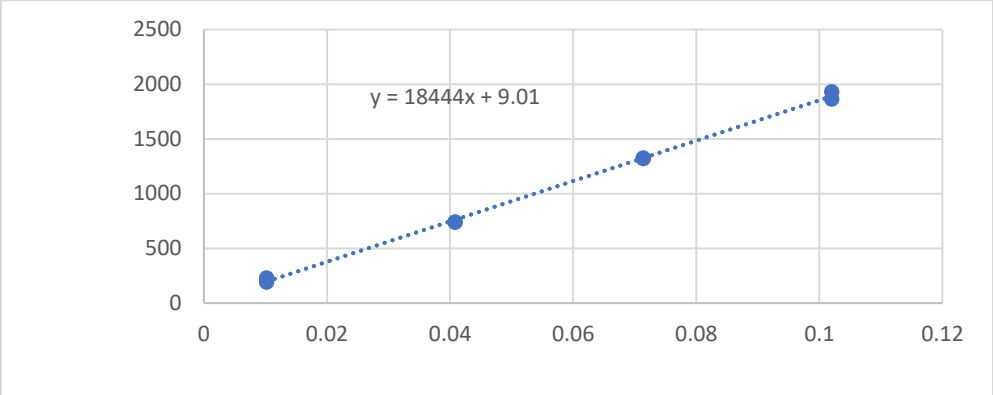

Figure A.5: Relationship between BE concentration (mg/mL) and peak area as determined by HPLC.

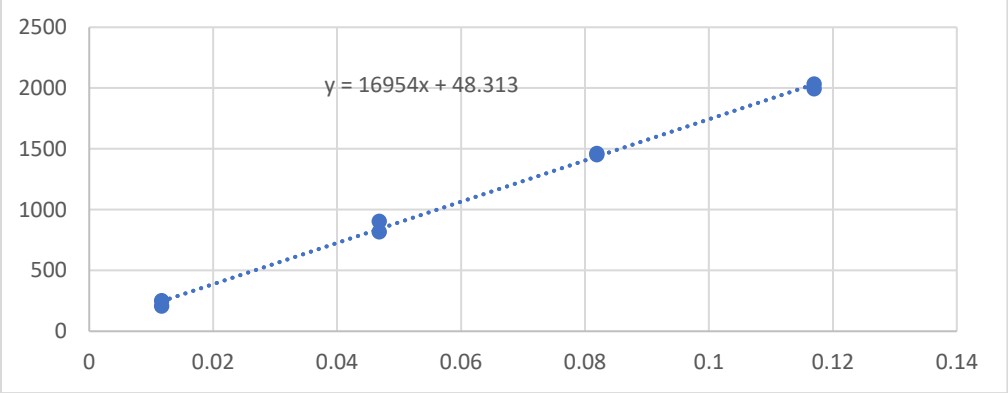

Figure A.6: : Relationship between BA concentration (mg/mL) and peak area as determined by HPLC.

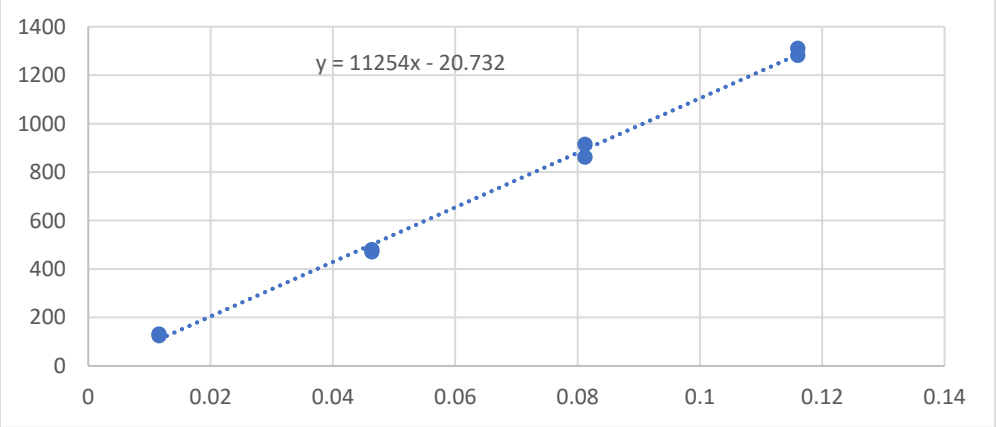

Figure A.7: Relationship between TE concentration (mg/mL) and peak area as determined by HPLC.

Table A.7: HPLC retention times, peak areas, corresponding concentrations calculated from standard curve of BE, and entrapment efficiencies of ethosome formulations used in optimization study.

Formulation	RT	Peak Area	Conc (mg/mL)	EE %	Avg EE%	Std Dev
A1	4.209	68.1	0.027990157	98.62117		
A2	4.173	70.9	0.029592537	98.51294		
A3	4.171	86.1	0.038291175	98.07582	98.40331	0.288732
B1	4.200	1141	0.641988097	68.83553		
B2	4.179	184.5	0.094603411	95.81401		
B3	4.180	159.8	0.080468124	96.84439	96.3292	0.728588
C1	4.193	726.9	0.40500744	85.05508		
C2	4.172	100.2	0.046360307	97.84371		
C3	4.178	55.3	0.020664988	99.01595	93.97158	7.74413
D1	4.182	285.7	0.152518027	92.17856		
D2	4.183	430.9	0.235612911	89.71123		
D3	4.181	337.4	0.182104841	91.87032	91.25337	1.344398
E1	4.181	153.2	0.076691084	96.24063		
E2	4.189	211.8	0.110226622	94.77599		
E3	4.182	145.3	0.072170081	96.26062	95.75908	0.85144
F1	4.172	106.7	0.050080119	97.79383		
F2	4.182	101.8	0.047275953	97.94452		
F3	4.177	121.7	0.058664301	96.86287		
F4	4.185	78.6	0.033999084	98.381		
F5	4.191	89.7	0.040351379	98.2902		
F6	4.174	130.7	0.063814811	96.69353	97.66099	0.71907
G1	4.188	492.8	0.271036969	88.2668		
G2	4.182	290.2	0.155093281	92.57927		
G4	4.182	308.7	0.16568044	91.41552		
G4	4.176	375.5	0.203908664	89.64931		
G5	4.209	683.4	0.380113311	80.80236		
G6	4.188	375.8	0.204080348	89.31517	88.6714	4.153502
H1	4.179	434.6	0.237730342	88.89111		
H2	4.181	209.5	0.108910381	94.6873		
H3	4.183	110.1	0.052025867	97.38563	93.65468	4.34039
I1	4.164	39.7	0.011737438	99.4384		
I2	4.191	83.9	0.037032162	98.1106		
I3	4.209	88.355	0.039581664	98.48925	98.67942	0.68402

Table A.8: HPLC peak areas, corresponding concentrations calculated from standard curves of BE, BA, and TE, and entrapment efficiencies of formulations of ethosomes containing triterpenes.

BE-ethosomes	Peak Area	Conc (mg/mL)	EE%	Avg EE%	SD
1	153.2	0.076691084	96.24063		
2	211.8	0.110226622	94.77599		
3	145.3	0.072170081	96.26062	95.75908	0.85144
BA-ethosomes					
1	1066.6	0.120123511	93.99382		
2	1243.3	0.140968149	92.95159		
3	1036.7	0.116596319	94.17018	93.7052	0.658574
TE-ethosomes					
1	701.5	0.128351164	93.61437		
2	755.8	0.138001066	93.23524		
3	747.8	0.13657935	93.17103	93.34021	0.239586

Table A.9: HPLC peak areas and corresponding concentrations calculated from standard curves of BE, BA, and TE of final solutions filtered through 0.8 μm prior to cell treatments.

Compound	Peak Area	Conc (mg/mL)
Betulin	14472.9	1.889935746
Betulinic Acid	12449.9	1.762877473
Triterpene Extract	7791	1.672851797

MTT Assay Data (Anti-melanoma Effect)

Relative Cell Viability = $(ABS_{sample} - ABS_{blank})/(ABS_{control} - ABS_{blank})*100$

ABS_{blank} = average of 3 blank wells $ABS_{control}$ = average of 3 control wells

Table A.10: ABS570 values from MTT assay for determination of cell viability of B16-F10 cells treated with ethosomal-BE, ethosomal-BA, and ethosomal-TE for 48 hours.

	Eth-BE			**Eth-BA**			**Eth-TE**		
	ABS	Corrected	% Viability	ABS	Corrected	% Viability	ABS	Corrected	% Viability
0.1 µM	0.955	0.840667	76.93716	1.057	0.942667	86.27212	0.917	0.814333	70.40347
	0.871	0.756667	69.24955	0.976	0.861667	78.85907	0.946	0.843333	72.91068
	0.773	0.658667	60.28067	0.82	0.705667	64.58207	1.207	1.104333	95.47553
Avg			**68.82246**			**76.57109**			**79.59656**
SD			8.336456			11.02455			13.80861
1 µM	0.541	0.426667	39.04822	0.597	0.482667	44.17329	0.815	0.712333	61.58502
	0.446	0.331667	30.3539	0.407	0.292667	26.78465	0.693	0.590333	51.03746
	0.686	0.571667	52.3185	0.552	0.437667	40.05493	0.894	0.791333	68.415
Avg			**40.57354**			**37.00429**			**60.34583**
SD			11.06146			9.086862			8.75479
10 µM	0.48	0.365667	33.46555	0.426	0.311667	28.52351	0.722	0.619333	53.54467
	0.396	0.281667	25.77794	0.372	0.257667	23.58148	0.679	0.576333	49.82709
	0.455	0.340667	31.17757	0.415	0.300667	27.5168	0.844	0.741333	64.09223
Avg			**30.14035**			**26.5406**			**55.82133**
SD			3.947367			2.61164			7.400062
20 µM	0.408	0.293667	26.87617	0.416	0.301667	27.60832	0.704	0.601333	51.98847
	0.387	0.272667	24.95426	0.408	0.293667	26.87617	0.695	0.592333	51.21038
	0.523	0.408667	37.40087	0.467	0.352667	32.2758	0.73	0.627333	54.23631
Avg			**29.74377**			**29.57598**			**52.47839**
SD			6.700513			3.818117			1.571333

Table A.11: Sample microplate ABS570 readings from PowerWave XS Microplate Spectrophotometer for 1, 10, and 20 µM ethosomal solutions of BE and BA (light grey), solvent control (dark grey), and blank (cross-hatching)

0.04	0.04	0.041	0.04	0.04	0.041	0.04	0.04	0.041	0.041	0.041	0.04
0.045	0.408	0.48	0.541	0.955	1.534	1.585	1.176	1.133	1.32	1.643	0.041
0.044	0.387	0.396	0.446	0.871	1.063	1.268	0.952	0.798	1.518	0.968	0.045
0.048	0.523	0.455	0.686	0.773	1.463	1.109	1.112	0.98	1.33	0.99	0.046
0.048	0.416	0.426	0.597	1.057	~~0.111~~	0.867	0.663	0.797	1.3	1.261	0.049
0.05	0.408	0.372	0.407	0.976	~~0.117~~	0.746	0.841	0.87	1.255	1.205	0.05
0.051	0.467	0.415	0.552	0.82	~~0.115~~	1.035	1.022	1.157	1.438	1.155	0.051
0.06	0.052	0.051	0.051	0.052	0.052	0.052	0.055	0.059	0.052	0.052	0.051

Table A.12: ABS570 values of wells containing formazan from MTT assay for determination of cell viability of B16-F10 cells treated with ethosomal-BE, ethosomal-BA, and ethosomal-TE for 48 hours.

	BE			**BA**			**TE**		
	ABS	Corrected	% Viability	ABS	Corrected	% Viability	ABS	Corrected	% Viability
0.1 µM	0.826	0.718333	93.04832	0.781	0.722	93.52332	0.503	0.407	79.36307
	0.779	0.671333	86.96023	0.653	0.545333	70.63899	0.538	0.442	86.1879
	0.666	0.558333	72.32293	0.892	0.784333	101.5975	0.627	0.531	103.5425
Avg			**84.11049**			**88.58661**			**89.69782**
SD			10.65252			16.05884			12.46598
1 µM	0.814	0.735	63.78365	0.987	0.908	78.79667	0.861	0.782	67.86233
	0.735	0.656	56.92799	0.847	0.768	66.6474	1.076	0.997	86.52013
	0.955	0.876	76.01969	0.816	0.737	63.95721	0.85	0.771	66.90774
Avg			**65.57711**			**69.80043**			**73.7634**
SD			9.671384			7.906236			11.05796
10 µM	0.713	0.634	55.01882	0.656	0.577	50.07233	1.072	0.993	86.17301
	0.736	0.657	57.01477	0.812	0.733	63.61008	0.734	0.655	56.84121
	0.775	0.696	60.39921	0.822	0.743	64.47789	0.873	0.794	68.90369
Avg			**57.4776**			**59.38677**			**70.6393**
SD			2.719891			8.078201			14.74272
20 µM	0.607	0.528	45.82009	0.535	0.456	39.57189	0.541	0.462	40.09258
	0.521	0.442	38.35697	0.688	0.609	52.84931	0.493	0.414	35.92711
	0.508	0.429	37.22882	0.569	0.49	42.52243	0.506	0.427	37.05526
Avg			**40.46863**			**44.98121**			**37.69165**
SD			4.668703			6.971845			2.154417

Table A.13: Microplate ABS570 readings from PowerWave XS Microplate Spectrophotometer for 1, 10, and 20 µM ethanolic solutions of BE, BA, and TE (light grey), solvent control (dark grey), and blank (cross-hatching).

0.04	0.04	0.041	0.041	0.042	0.041	0.041	0.041	0.042	0.042	0.041	0.041
0.047	0.588	0.607	0.713	0.814	2.148	1.695	1.83	2.007	1.238	1.04	0.041
0.044	0.603	0.521	0.736	0.735	2.581	1.921	3.132	2.137	1.941	1.277	0.045
0.047	0.501	0.508	0.775	0.955	2.266	2.153	3.297	1.999	1.475	1.377	0.046
0.048	0.07	0.767	0.656	0.987	0.079	0.639	0.541	1.072	0.861	1.625	0.051
0.127	0.704	0.758	0.812	0.847	0.076	0.502	0.493	0.734	1.076	2.845	0.05
0.051	0.83	0.681	0.822	0.816	0.082	0.62	0.506	0.873	0.85	2.605	0.052
0.053	0.053	0.054	0.053	0.053	0.053	0.052	0.053	0.053	0.053	0.053	0.052

Determination of IC_{50} values for ethosomal triterpenes (ED50plus V1.0 Software)

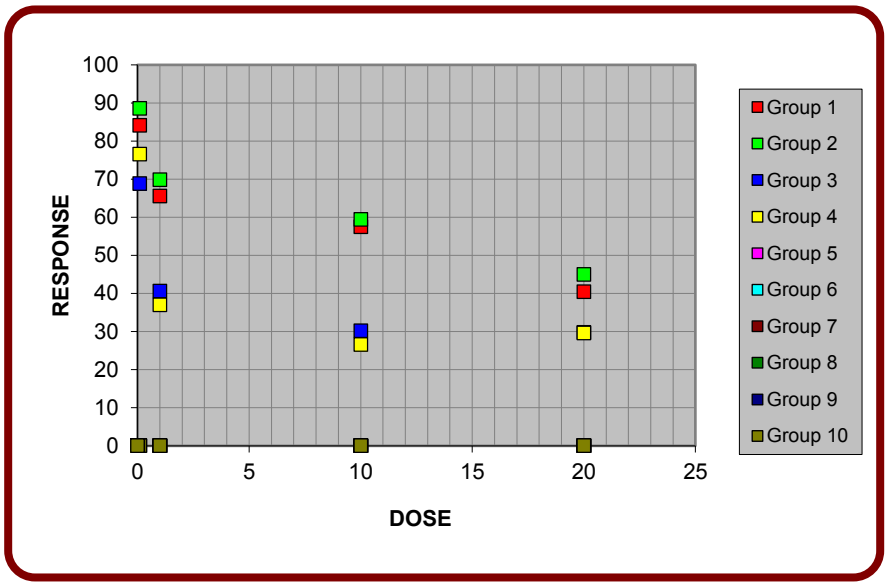

Figure A.8: Dose response curves generated by ED50plus V1.0 software used to calculate IC_{50} values for all treatments. Group 1 = BE, Group 2 = BA, Group 3 = TE, Group 4 = E-BE, Group 5 = E-BA, Group 6 = E-TE.

Table A.14: Relative cell viabilities of B16-F10 cells (response) corresponding to each treatment (dose) as determined by MTT assay after 48 hour treatment.

	Response					
Dose	BE	BA	TE	E-BE	E-BA	E-TE
0.1 µM	84.11	88.58661	89.69782	68.82246	76.57109	79.59656
1 µM	65.57	69.80043	73.7634	40.57364	37.00429	60.34583
10 µM	57.4776	59.38677	70.6393	30.14035	26.5406	55.82133
20 µM	40.46863	44.98121	37.69165	29.74377	29.57598	52.47839
IC_{50} (µM)	**14.381388**	**16.413293**	**15.933653**	**2.4296773**	**3.0737834**	**20.082995**

Cellular Tyrosinase Activity Data (Anti-melanogenic Effect)

Relative Tyrosinase Activity = $(ABS_{sample} - ABS_{blank})/(ABS_{control} - ABS_{blank})*100$

ABS_{blank} = average of 3 blank wells $ABS_{control}$ = average of 3 control wells

Table A.15: ABS490 values of wells containing dopaquinone, the product of L-DOPA oxidation by tyrosinase as measure of relative tyrosinase activity in B16-F10 cells treated with BE, BA, and TE for 48 hours in the presence of 100 μM IBMX.

	ABS	Corrected	% Activity
0.01 μM BE	0.3	0.239333	79.60095
	0.292	0.231333	76.94019
	0.326	0.265333	88.24842
		Avg	**81.59652**
		SD	5.912338
0.01 μM BA	0.339	0.278333	92.57216
	0.277	0.216333	71.95127
	0.281	0.220333	73.28165
		Avg	**79.26836**
		SD	11.54061
0.01 μM TE	0.285	0.224333	74.61203
	0.303	0.242333	80.59874
	0.344	0.283333	94.23513
		Avg	**83.14863**
		SD	10.05699

Table A.16: Microplate ABS490 readings from PowerWave XS Microplate Spectrophotometer for 1 nM BE, BA, and TE ethanolic solutions and 1-500 μM KA (light grey), solvent controls (dark grey), and blank (cross-hatching).

0.043	0.041	0.042	0.041	0.042	0.042	0.042	0.042	0.043	0.044	0.042	0.046
0.049	0.3	0.334	0.323	0.342	0.352	0.285	0.302	0.243	0.246	0.181	0.042
0.047	0.27	0.274	0.318	0.311	0.213	0.303	0.301	0.231	0.262	0.216	0.054
0.055	0.346	0.347	0.42	0.323	0.325	0.344	0.373	0.261	0.311	0.241	0.047
0.052	0.339	0.403	0.381	0.42	0.06	0.371	0.372	0.286	0.166	0.124	0.058
0.06	0.277	0.403	0.375	0.401	0.062	0.384	0.351	0.261	0.184	0.131	0.055
0.053	0.281	0.323	0.272	0.371	0.06	0.351	0.353	0.245	0.159	0.144	0.061
0.062	0.057	0.058	0.058	0.059	0.061	0.059	0.059	0.058	0.058	0.057	0.06

Table A.17: ABS490 values of wells containing dopaquinone, the product of L-DOPA oxidation by tyrosinase as measure of relative tyrosinase activity in B16-F10 cells treated with 1-500 μM KA for 48 hours in the presence of 100 μM IBMX.

	ABS	Corrected	% Activity
1 μM KA	0.371	0.310333	103.2152
	0.384	0.323333	107.5389
	0.351	0.290333	96.5633
		Avg	**102.4391**
		SD	5.528818
10 μM KA	0.372	0.311333	103.5478
	0.351	0.290333	96.5633
	0.353	0.292333	97.22849
		Avg	**99.11319**
		SD	3.854851
100 μM KA	0.286	0.225333	74.94462
	0.261	0.200333	66.62975
	0.245	0.184333	61.30823
		Avg	**67.62753**
		SD	6.872735
250 μM KA	0.166	0.105333	35.03323
	0.184	0.123333	41.01994
	0.159	0.098333	32.70506
		Avg	**36.25274**
		SD	4.289487
500 μM KA	0.124	0.063333	21.06424
	0.131	0.070333	23.3924
	0.144	0.083333	27.71614
		Avg	**24.05759**
		SD	3.37547